

A Geologic Field Guide to S P Mountain and its Lava Flow, San Francisco Volcanic Field, Arizona



Open-File Report 2021–1072

Cover. Photograph of S P Mountain, Arizona. Photograph by Amber Gullikson, U.S. Geological Survey.

A Geologic Field Guide to S P Mountain and its Lava Flow, San Francisco Volcanic Field, Arizona

By Amber L. Gullikson, M. Elise Rumpf, Lauren A. Edgar, Laszlo P. Keszthelyi,
James A. Skinner, Jr., and Lisa Thompson

Open-File Report 2021–1072

U.S. Department of the Interior
U.S. Geological Survey

U.S. Geological Survey, Reston, Virginia: 2021

For more information on the USGS—the Federal source for science about the Earth, its natural and living resources, natural hazards, and the environment—visit <https://www.usgs.gov> or call 1–888–ASK–USGS (1–888–275–8747).

For an overview of USGS information products, including maps, imagery, and publications, visit <https://store.usgs.gov>.

Any use of trade, firm, or product names is for descriptive purposes only and does not imply endorsement by the U.S. Government.

Although this information product, for the most part, is in the public domain, it also may contain copyrighted materials as noted in the text. Permission to reproduce copyrighted items must be secured from the copyright owner.

Suggested citation:

Gullikson, A.L., Rumpf, M.E., Edgar, L.A., Keszthelyi, L.P., Skinner, J.A., Jr., and Thompson, L., 2021, A geologic field guide to S P Mountain and its lava flow, San Francisco Volcanic Field, Arizona: U.S. Geological Survey Open-File Report 2021–1072, 37 p., <https://doi.org/10.3133/ofr20211072>.

ISSN 2331-1258 (online)

Acknowledgments

We are grateful to Greg Vaughan (USGS) and Mark Salvatore (Northern Arizona University) for their insightful comments which have greatly improved this report.

Contents

Acknowledgments	iii
Introduction.....	1
A Brief Tour of Volcanism Across the Solar System.....	1
Mercury.....	2
Venus.....	2
Earth.....	2
The Moon	4
Mars.....	4
Meteorites.....	6
Io.....	7
Summary of Volcanism in the Solar System.....	7
A Brief Geologic History of the Colorado Plateau and San Francisco Volcanic Field	8
The Physiographic Regions of Arizona	8
Raising the Colorado Plateau	8
Rock Ages of the Colorado Plateau Province.....	9
San Francisco Volcanic Field.....	10
Fault Systems within the San Francisco Volcanic Field.....	11
Sources of Volcanic Rock Compositions	12
Distributed Volcanism and Associated Volcanic Features.....	12
Distributed Volcanic Fields and Clusters	12
Eruption Styles.....	13
Lava Flows.....	14
S P Mountain and its Lava Flow	14
The Age of S P Mountain.....	14
Dimensions of S P Mountain and General Features.....	14
Dimensions of S P Mountain Lava Flow and General Features.....	14
Lava Flow Emplacement Theories	16
S P Graben	16
Getting to S P Mountain.....	17
Disclaimer	18
Stop 1. Source of the Lava Flow.....	18
Stop 2. At the Intersection of the Road and Lava Flow	23
Stop 3. Lava Flow	24
Stop 4. The Rim of S P Mountain.....	27
Stop 5. Graben.....	31
Questions for Discussion at the End of the Field Trip	34
References.....	34

Figures

1. Satellite images of volcanic features on Venus	3
2. Photograph of flood lavas in Mare Imbrium as seen from orbit	4
3. Satellite image of lunar volcanism.....	5
4. Satellite image of an aerial view of Olympus Mons	5
5. Satellite image of lava flows associated with the Arsia Mons volcanic complex	5
6. Satellite image of what is presumed to be volcanic cones located in the Coprates Chasma region of the Valles Marineris canyon system.....	6
7. Satellite image of an eroded portion of the Medusae Fossae Formation, a unit thought to have formed from pyroclastic flows or volcanic ash deposits.....	6
8. Photograph of a cumulate eucrite meteorite.....	6
9. Satellite image of Amirani (an active volcano on Io) and its flow field	7
10. Satellite image comparing S P Mountain to a satellite image of a volcano on Mars.....	7
11. Map of Arizona showing the three main physiographic provinces that compose Arizona	8
12. Map of the physiographic provinces in Utah, Colorado, Arizona, and New Mexico	9
13. Geologic block diagram showing the surface and subsurface geology of the Flagstaff area.....	10
14. Digital elevation model of the San Francisco Volcanic Field	11
15. Illustration of the extent of the San Francisco Volcanic Field and its silicic and intermediate vents, major fault systems, and the northern extent of rim basalts	12
16. Satellite image of the field site.....	13
17. Photograph of an oblique view of S P Mountain, showing the volcano's dimensions ...	14
18. Photographs of lava flow near S P Mountain showing the contrast between surface texture 1 and 2.....	15
19. Photograph of an agglutinated mound that was transported away from the vent downstream.....	16
20. Photographs of the S P Mountain lava flow showing the graben and spillover.....	17
21. Schematic cross section of a typical tephra cone	17
22. Satellite image of S P Mountain, highlighting the locations of the first four stops of the guidebook	18
23. Photograph of the source of the lava from stop 1.....	19
24. Photograph looking north from stop 1.....	19
25. Photograph looking west from stop 1.....	20
26. Photographs of a lava bomb at stop 1.....	20
27. Photograph looking north toward the lava flow at stop 1.....	21
28. Photograph of the lava flow and onlapping tephra at stop 1	21
29. Photographs of two types of tephra at stop 1.....	22
30. Photograph looking south at the contact point between S P Mountain and an older tephra cone to the west at stop 2	23
31. Looking south at S P Mountain and the source of the lava flow standing on the road near stop 2	23
32. Photograph taken on the vegetated portion of the lava flow at stop 3	24
33. Photograph of surface texture 1 at stop 3.....	25
34. Photograph of a blocky and unvegetated lava flow, looking south from stop 3	25
35. Photographs of the S P Mountain lava flow at stop 3	26
36. Photographs of polygonal pavement at stop 3	26

37.	Photograph taken at stop 4 of the rim of S P Mountain looking east	27
38.	Photograph taken at stop 4 from the rim of S P Mountain looking north	27
39.	Photograph of a red agglutinated piece of volcanic rock taken on the rim of S P Mountain at stop 4	28
40.	Photograph of smaller lapilli welded onto a lava bomb taken along the rim of S P Mountain at stop 4	28
41.	Photograph of compressional bands on a volcanic rock taken along the rim of S P Mountain at stop 4	28
42.	Photograph taken at stop 4 looking northwest toward the S P Mountain lava flow	29
43.	Photograph taken at stop 4 looking northeast	29
44.	Photograph taken at stop 4 on the rim of S P Mountain looking southwest	30
45.	Photograph taken at stop 4 on the rim of S P Mountain looking to the south at Colton Crater	30
46.	Satellite image showing how to get to stop 5	31
47.	Photograph taken at stop 5 on the floor of the graben with the S P Mountain lava flow to the east	31
48.	Photographs of agglutinated transported material located within the S P Mountain lava flow, taken at one of the lobes that entered the graben	32
49.	Photograph at stop 5 between the Kaibab Limestone and the S P Mountain lava flow	32
50.	Photograph of the S P Mountain lava flow lobe, taken standing on the Kaibab Limestone looking south at stop 5	33
51.	Photograph of the S P Mountain lava flow on the left side with S P Mountain in the background, taken on top of an agglutinated mound transported by the S P Mountain lava flow	33

Tables

1.	Volcanic eruption classification based on erupted volume	2
2.	Simplified volcanic rock classification based on major minerals and silica content	2
3.	Particle size classification for volcanic and sedimentary rocks	2

Conversion Factors

U.S. customary units to International System of Units

Multiply	By	To obtain
	Length	
foot (ft)	0.3048	meter (m)
mile (mi)	1.609	kilometer (km)

International System of Units to U.S. customary units

Multiply	By	To obtain
	Length	
centimeter (cm)	0.3937	inch (in.)
millimeter (mm)	0.03937	inch (in.)
meter (m)	3.281	foot (ft)
kilometer (km)	0.6214	mile (mi)
kilometer (km)	0.5400	mile, nautical (nmi)
meter (m)	1.094	yard (yd)
	Area	
square kilometer (km ²)	247.1	acre
square kilometer (km ²)	0.3861	square mile (mi ²)

Abbreviations

DEM	digital elevation model
GPS	global positioning system
HED	Howardite-eucrite-diogenite
NASA	National Aeronautics and Space Administration
OSL	Optically stimulated luminescence
USGS	U.S. Geological Survey

A Geologic Field Guide to S P Mountain and its Lava Flow, San Francisco Volcanic Field, Arizona

By Amber L. Gullikson,¹ M. Elise Rumpf,¹ Lauren A. Edgar,¹ Lazlo P. Keszthelyi,¹ James A. Skinner, Jr.,¹ and Lisa Thompson²

Introduction

We created this guide to introduce the user to the San Francisco Volcanic Field as a terrestrial analog site for planetary volcanic processes. For decades, the San Francisco Volcanic Field has been used to teach scientists to recognize the products of common types of volcanic eruptions and associated volcanic features. The volcanic processes and products observed in this volcanic field are like those observed on lunar and Martian surfaces. As a result, this region has been a favored location for training National Aeronautics and Space Administration astronauts and engineers since the Apollo missions.

Though the San Francisco Volcanic Field has more than 600 volcanic vents and flows, this guide will focus on S P Mountain (known locally as S P Crater, located ~30 miles north of Flagstaff, Arizona), one of the best preserved and most accessible of the volcanic cones and lava flows. S P Mountain presents both major types of basaltic eruptions—explosive and effusive—as well as some commonly associated tectonic landforms.

We assume that the user has a basic understanding of geologic concepts and terminology. For more specialized terminology, we include tables showing the classification scheme for lava compositions, styles of eruptions, and tephra sizes (tables 1, 2, and 3). If a further introduction or refresher in volcanological terminology is desired, we suggest reviewing such terms on the U.S. Geological Survey Volcano Science Center's online glossary (<https://volcanoes.usgs.gov/vsc/glossary/>).

One term requires clarification at the start of this guide—the term cinder. The terms cinder and cinder cone are widely used to describe the material and edifice produced by lava fountains. However, the term comes from the mining and construction industries and has no clear or formal definition. The international committees in geology and volcanology have chosen the term tephra to be the general term to describe pyroclasts (material ejected through a volcanic explosion or from a volcanic vent). Therefore, in this guide, we use the term tephra rather than cinder.

This guide is outlined as follows:

- A brief tour of volcanism across the solar system
- A brief geologic history of the Colorado Plateau and San Francisco Volcanic Field
- Background on distributed volcanism and S P Mountain
- Driving directions and field stops
- Questions for discussion

Each field stop includes a brief description, learning goals, tasks, and a summary of key points. At the end of the field guide are discussion points and questions that will ask the user to consider what they have observed and learned and how such knowledge can be used to better our understanding of geologic processes on other planetary bodies.

Upon the completion of this field guide, we expect the user to:

- Have a basic understanding of the volcanic processes relevant to S P Mountain and its lava flow.
- Be able to identify different volcanic textures that are associated with tephra cones.
- Be aware of the different observations one can make at different scales (for example, observing lava flow morphology from aerial or satellite imagery versus tephra characteristics in the field).

A Brief Tour of Volcanism Across the Solar System

Volcanism is one of the fundamental geologic processes that have shaped our solar system and is indicated by the prevalence of basalt, a magnesium- and iron-rich volcanic rock, on planetary surfaces (for example, Cattermole, 1989; Hodges and Moore, 1994; Lopes and Gregg, 2004; Gregg and others, 2020). Here, we briefly tour the planets, moons, and asteroids of our solar system that show evidence of volcanism to have occurred at some time in their history. First, we begin with Mercury, the closest planet to the Sun.

¹U.S. Geological Survey.

²Northern Arizona University.

2 A Geologic Field Guide to S P Mountain and its Lava Flow, San Francisco Volcanic Field, Arizona

Table 1. Volcanic eruption classification based on erupted volume.

[Volcanologists have developed many classification schemes for types of volcanic eruptions, but the international standard relies on names derived from a volcano that best typifies each class of eruption. This classification was made quantitative by Newhall and Self (1982) using the logarithmic volcanic explosivity index (VEI) presented below. km³, cubic kilometer]

Name	Description	VEI	Erupted volume (km ³)
Hawaiian	Sustained lava fountains that can feed lava flows and build cones of tephra.	0–1	<0.001
Strombolian	Intermittent bursts or jets of bubble-rich magma that can lead to modest edifices.	1–3	<0.1
Vulcanian	Intermittent gas-rich explosions with a mix of pyroclasts and lithics from wall-rocks; limited edifice building.	2–4	0.001–1
Plinian	Violent explosive eruptions that produce ash-sized particles; often leads to caldera formation.	4–8	0.1– >1000

Table 2. Simplified volcanic rock classification based on major minerals and silica content.

[Although much more sophisticated distinctions can be made between rocks once they are analyzed in the laboratory, in the field broader categories are typically used. SiO₂ wt.%, weight percent silica dioxide]

Extrusive name	Intrusive name	Major minerals	Silica content (SiO ₂ wt.%)
Komatiite	Peridotite	Olivine and pyroxene	<45
Basalt	Gabbro	Plagioclase, pyroxene, and ± olivine	45–52
Andesite	Diorite	Plagioclase, pyroxene/amphibole/biotite, and ± quartz	52–63
Rhyolite	Granite	K-feldspar, quartz, plagioclase, and ± biotite/amphibole	>63

Table 3. Particle size classification for volcanic and sedimentary rocks.

[mm, millimeters]

Diameter (mm)	Tephra name	Sediment name
>64	Bomb	Cobble or boulder
2–64	Lapilli	Gravel
<2	Ash	Sand, silt, and clay

Mercury

Although evidence for volcanism on Mercury is ample, its lavas are ancient and have been subjected to eons of meteorite bombardment. For this reason, direct volcanological studies on Mercury are nearly impossible (Solomon and others, 2018).

Venus

Under its thick clouds, Venus' surface is dominated by geologically young volcanic rocks. These include familiar landforms such as shield volcanoes (fig. 1A), cones (fig. 1B), and lava flows (fig. 1C), as well as less familiar landforms such as pancake domes (fig. 1D) and canali (fig. 1E). The morphology of the lava flows and chemical measurement from landers indicate that the surface of Venus is dominated by basaltic lavas, although some enigmatic features could have unusual compositions (for example, pancake dome [Carmenta Farra], see Lunar and Planetary Institute website, https://www.lpi.usra.edu/resources/stereo_atlas/HTDOCS/VPAN.HTM).

Earth

The Earth has the most diverse styles of eruption and lava composition compared to other planetary bodies discovered thus far. This is due, in part, to the diversity of geologic settings formed through shifting of Earth's tectonic plates. However, even on Earth, basalt is the most common lava and covers most of the ocean floors. Basalt is also a common product of volcanism associated with mantle plumes and continental rifting. Other lavas, such as andesite and rhyolite, are primarily associated with subduction zones or where magma storage leads to a change in chemistry (see U.S. Geological Survey Volcano Hazards website, https://volcanoes.usgs.gov/vhp/about_volcanoes.html, for more information on volcanoes).

Studies of active volcanoes on Earth are particularly important because they test physics-based models of volcanic processes. Once these models are tested, they can be extrapolated with some confidence to the conditions found elsewhere in the solar system, hence the importance

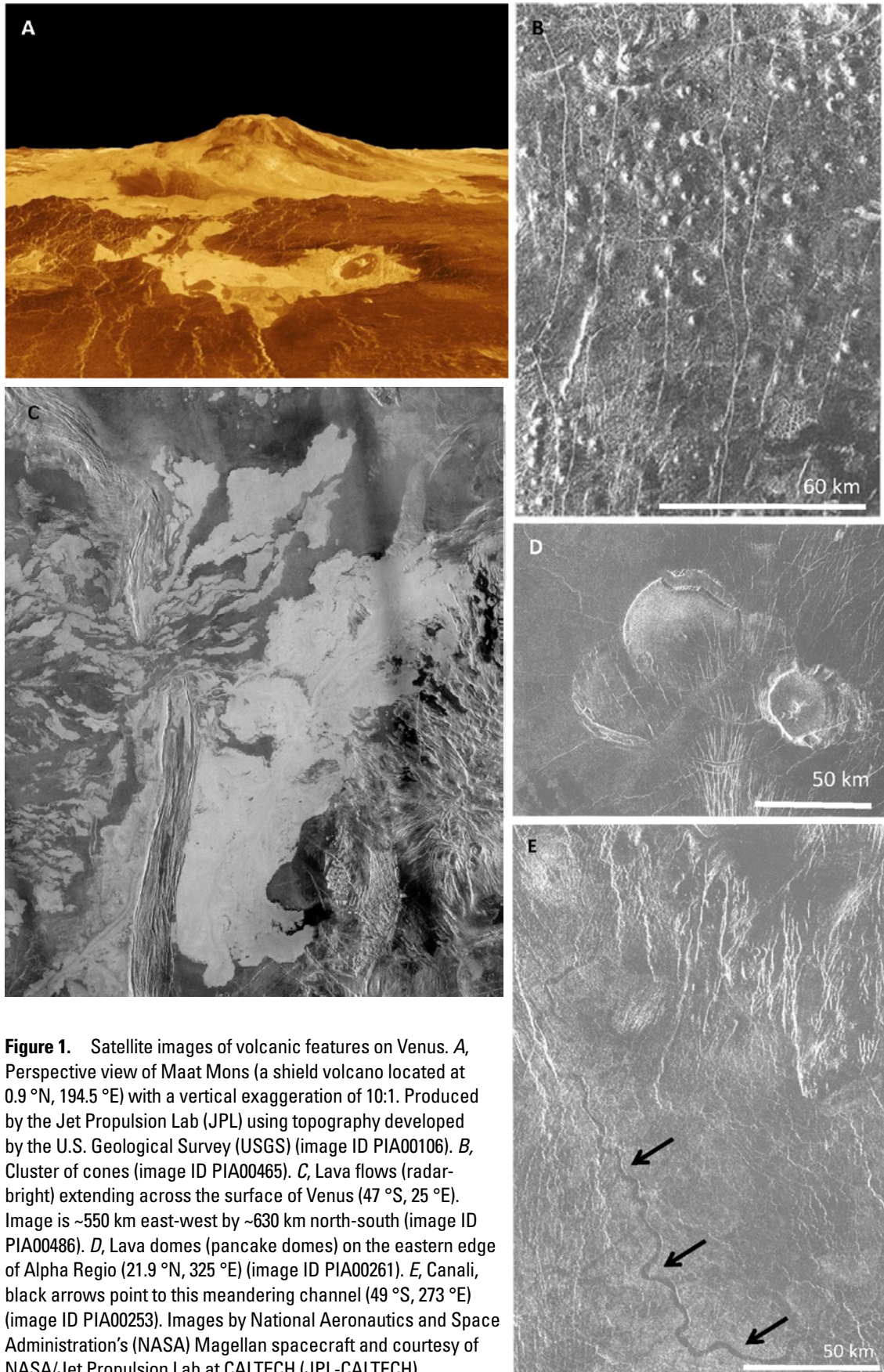


Figure 1. Satellite images of volcanic features on Venus. *A*, Perspective view of Maat Mons (a shield volcano located at 0.9°N , 194.5°E) with a vertical exaggeration of 10:1. Produced by the Jet Propulsion Lab (JPL) using topography developed by the U.S. Geological Survey (USGS) (image ID PIA00106). *B*, Cluster of cones (image ID PIA00465). *C*, Lava flows (radar-bright) extending across the surface of Venus (47°S , 25°E). Image is ~ 550 km east-west by ~ 630 km north-south (image ID PIA00486). *D*, Lava domes (pancake domes) on the eastern edge of Alpha Regio (21.9°N , 325°E) (image ID PIA00261). *E*, Canali, black arrows point to this meandering channel (49°S , 273°E) (image ID PIA00253). Images by National Aeronautics and Space Administration's (NASA) Magellan spacecraft and courtesy of NASA/Jet Propulsion Lab at CALTECH (JPL-CALTECH).

4 A Geologic Field Guide to S P Mountain and its Lava Flow, San Francisco Volcanic Field, Arizona

of terrestrial analogs. Overall, environmental changes (such as ambient temperature, gravity, and atmosphere) have only modest effects on the behavior of basaltic lava flows (for example, Keszthelyi, 1995; Keszthelyi and others, 2006); however, Earth's relatively thick atmosphere does have a major effect on how volcanic gases can expand and propel erupting material (Wilson and Head, 1981).

The Moon

The nearside of our Moon is riddled with large dark patches, many of which are basins formed by ancient meteorite impacts. These impacts were incredibly large and energetic and resulted in heavily fractured lunar crust. Magma ascended along such fractures and erupted basaltic lava onto the surface, which filled the low-lying impact basins. Additional volcanic landforms such as shield volcanoes, tephra deposits, and even silicic domes have also been observed on the lunar surface (Spudis, 2015).

The Moon's low gravity in comparison to Earth, has two main effects on volcanism and resulting volcanic features: first, lava flows are expected to be shorter and thicker because lower gravity leads to less force driving the flow downslope

(fig. 2). Second, pyroclasts are expected to travel farther, resulting in more areally expansive and thinner tephra deposits when compared to Earth (fig 3) (Wilson and Head, 1981).

Mars

Volcanism on Mars is widespread and has been extensively studied (Carr, 1973; Greeley and Spudis, 1981; Tanaka and others, 2014). The giant shield volcanoes that define the Tharsis Montes and surrounding regions, including the 27-km-tall (kilometer) Olympus Mons (the tallest volcano in the solar system), are perhaps the most famous. Although Olympus Mons has the same general shape as the largest volcano on Earth, the Hawaiian shield volcano Mauna Loa, it is approximately 100 times more voluminous and covers an area roughly equivalent to the State of Arizona (fig. 4). The massive volcanoes of Tharsis Montes are covered in thick lava flows and are surrounded by vast plains of lava (fig. 5). Though much of the evidence of older volcanism on Mars has been obscured by younger geologic activity, some younger lavas are remarkably well preserved. The younger lavas have exceptionally rough surfaces in both visible images and radar data (Keszthelyi and others, 2004, 2008; Harmon and others,

2012). Smaller tephra cones have also been found on the surface of Mars (fig. 6). Some of these features are thought to be the result of ground ice boiling under hot lava; however, their origin is often difficult to determine with certainty (Keszthelyi and others, 2008). The thinner atmosphere and lower gravity on Mars in comparison to Earth are expected to lead to wider dispersal of pyroclasts than on Earth (Wilson and Head, 1981). One such example is the Medusae Fossae Formation (fig. 7), a geologic unit that is interpreted to contain several kilometer-thick sequences of redeposited volcanic ash (Bradley and others, 2002; Kerber and others, 2013).

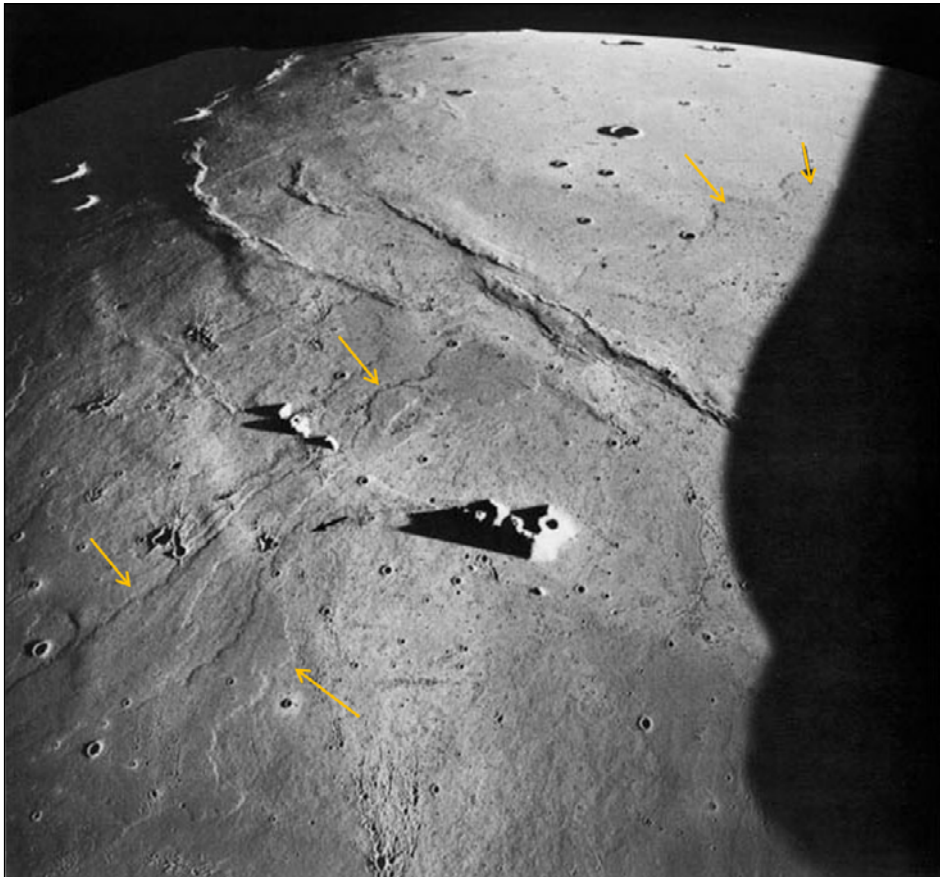


Figure 2. Photograph of flood lavas in Mare Imbrium as seen from orbit (Apollo image AS15 M 1555). Orange arrows point to lava flows. Photograph by National Aeronautics and Space Administration (NASA).

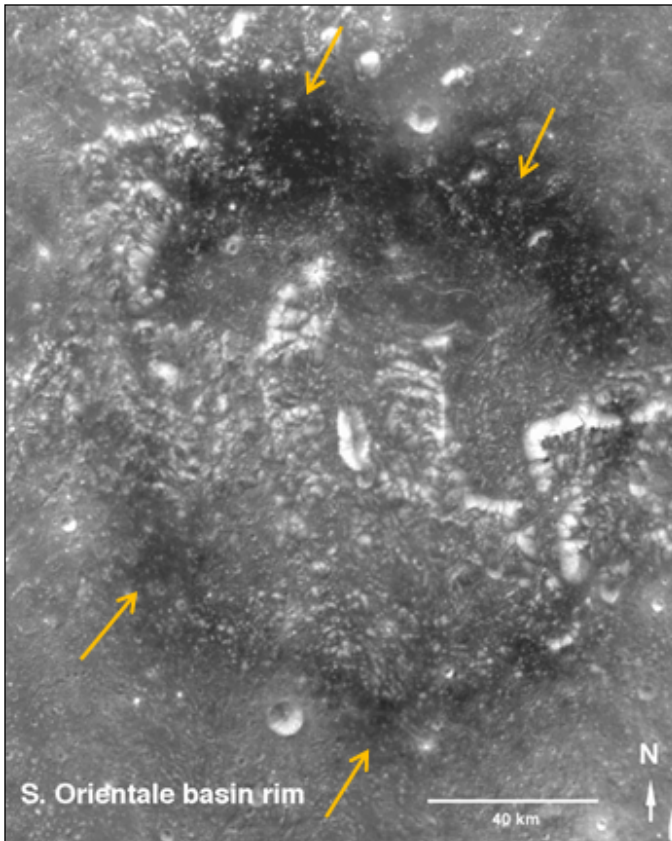


Figure 3. Satellite image of lunar volcanism, a ring-shaped or annular pyroclastic deposit on the southern rim of Orientale basin (30 °S, -97 °E). Orange arrows point to the deposit. Base map is from Clementine 750 nm images from orbits 203-204-205. Image by National Aeronautics and Space Administration (NASA), Jet Propulsion Lab (JPL), and the U.S. Geological Survey (USGS).

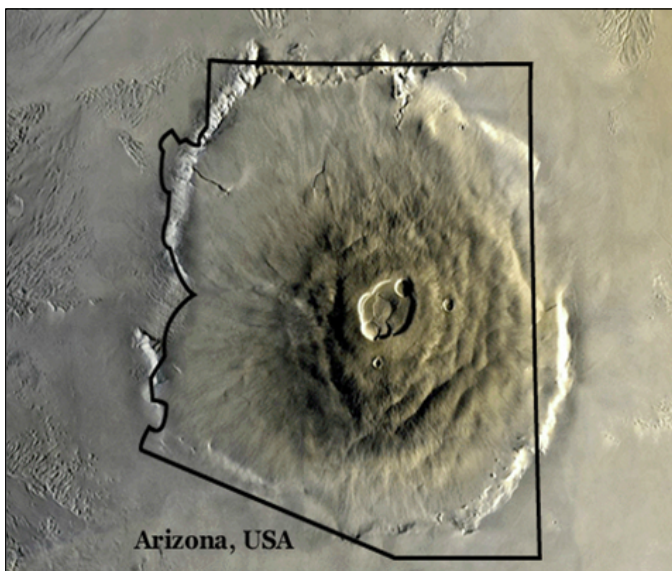


Figure 4. Satellite image of an aerial view of Olympus Mons (Image ID PIA02982) (18.7 °N, 226.0 °E), with the outline of the State of Arizona in black (<https://mars.nasa.gov/gallery/atlas/olympus-mons.html>). Image courtesy of National Aeronautics and Space Administration (NASA) and Jet Propulsion Lab at CALTECH (JPL-CALTECH).

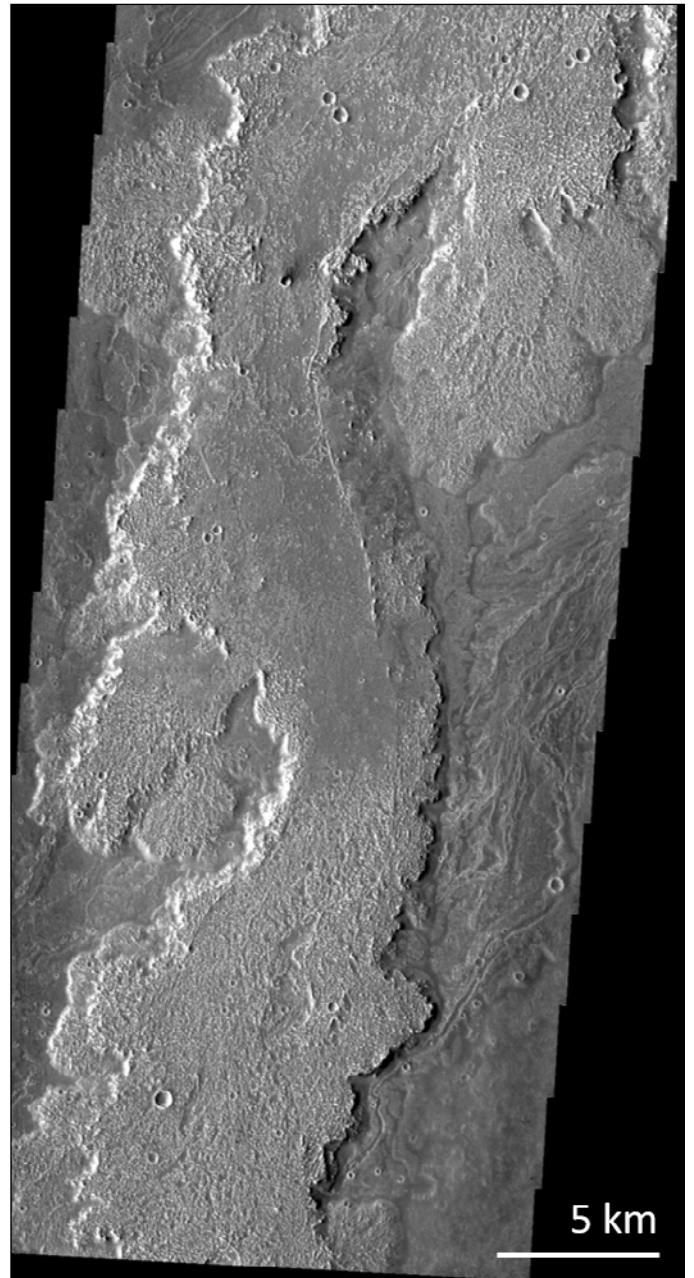


Figure 5. Satellite image of lava flows associated with the Arsia Mons volcanic complex (image ID PIA08023) (-23.4 °N, 241.4 °E) (Christensen and others, 2001). Image by the National Aeronautics and Space Administration (NASA), Jet Propulsion Lab at CALTECH (JPL-CALTECH), and Arizona State University.

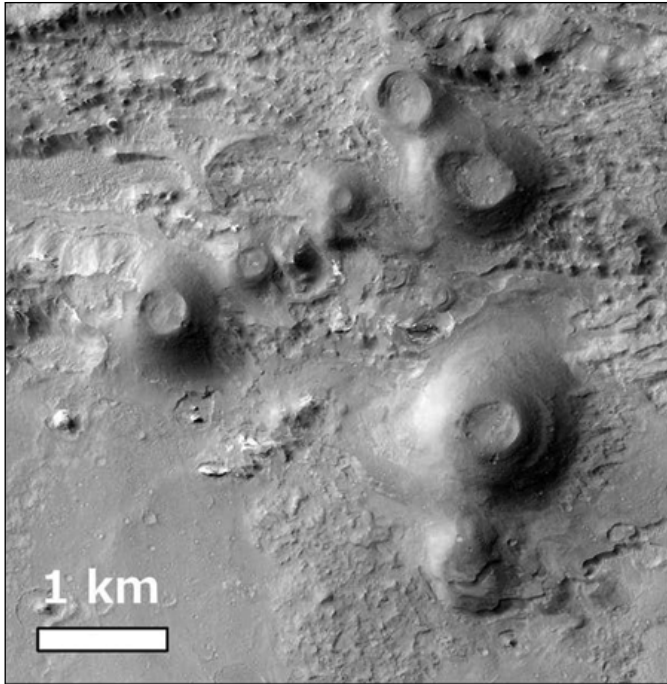


Figure 6. Satellite image of what is presumed to be volcanic cones located in the Coprates Chasma region of the Valles Marineris canyon system (HiRISE image ESP 034131 1670) (12.43 °S, 62.48 °W). Image by National Aeronautics and Space Administration (NASA), Jet Propulsion Lab (JPL), and the University of Arizona.

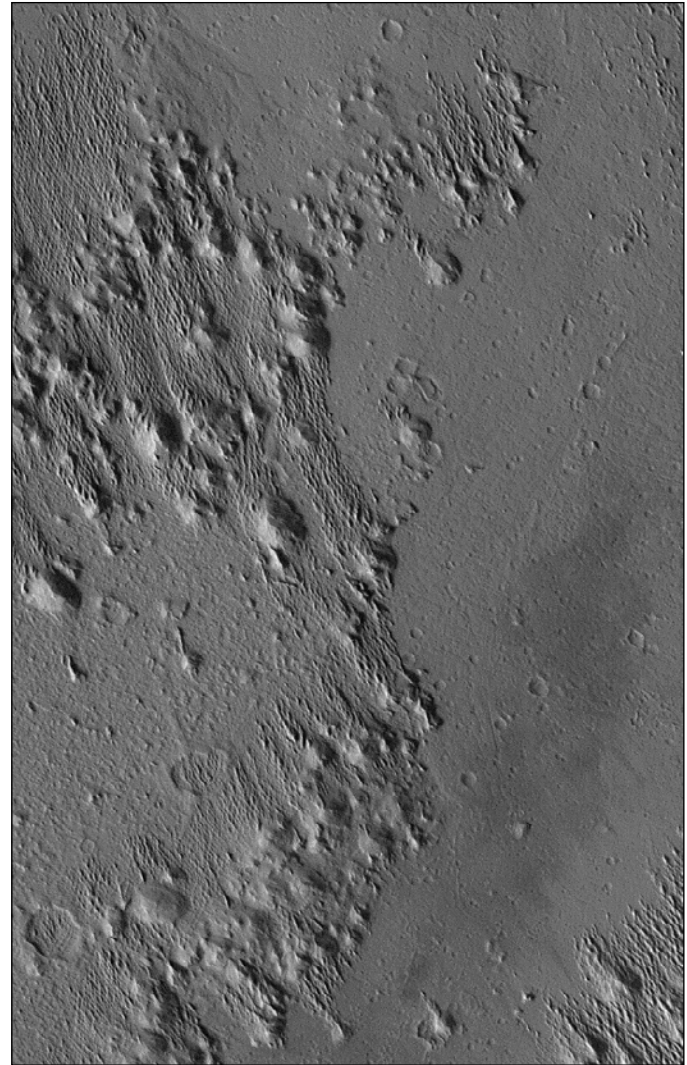


Figure 7. Satellite image of an eroded portion of the Medusae Fossae Formation (2.0 °N, 163.8 °W), a unit thought to have formed from pyroclastic flows or volcanic ash deposits, image is 3.0×4.7 kilometer in area (image ID PIA00801). Image by National Aeronautics and Space Administration (NASA), Jet Propulsion Lab (JPL), and Malin Space Science Systems.

Meteorites

Achondrites are a subclass of stony meteorites believed to have originated from other planets, moons, and asteroids in our solar system. This type of meteorite lacks chondrules (a spherical, millimeter-sized silicate inclusion found within chondrite meteorites) and exhibits igneous textures, which indicates that widespread melting occurred on its parent body (fig. 8) (Alexander and Wetherill, 2020). Meteorites derived from the asteroid Vesta (located in the asteroid belt between Mars and Jupiter) include rocks that have been through magmatic processes, indicating that some asteroids likely were volcanically active in their earliest histories (Jourdan and others, 2020). However, when the Dawn spacecraft visited Vesta in 2011, it found a surface too modified by a long history of impact cratering to retain volcanic morphologic features (Barnett and others, 2018) (<https://solarsystem.nasa.gov/missions/dawn/science/vesta/>).

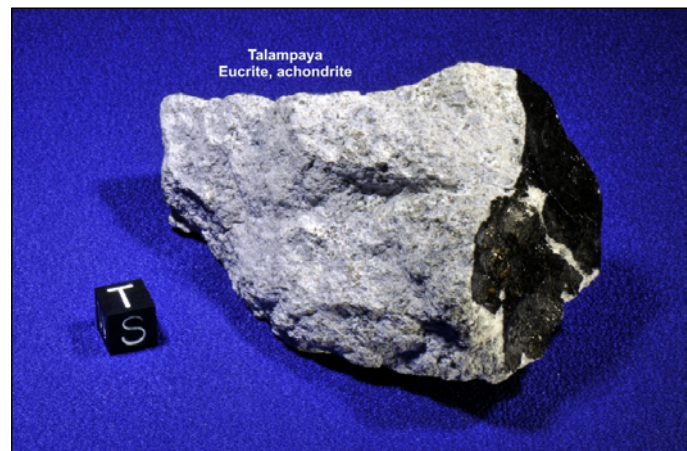


Figure 8. Photograph of a cumulate eucrite, a member of the HED (howardite-eucrite-diogenite) basaltic achondrite group thought to originate from the asteroid, Vesta. Cube is 1 centimeter across, used for scale. Photograph by Laurence Garvie, Arizona State University. Courtesy of the Arizona State University Center for Meteorite Studies (<https://meteorites.asu.edu/meteorites/talampaya>).

Io

In the outer solar system (beyond the asteroid belt), temperatures are low enough that most solid surface bodies are covered by ice, which obscures evidence of volcanism (though the melting, vaporization, and movement of these ices can produce cryovolcanism). One stunning exception is Io, the innermost of Jupiter's four largest moons. Tidal heating within Io escapes through more than 100 active volcanoes scattered across the surface. The ability to observe active volcanic eruptions on a body with the same gravity and lack of atmosphere as the Moon provides an opportunity to test volcanic models. The scale of the active lava flows on Io is larger than any modern flows on Earth. For example, the lava flow associated with Amirani patera is 530 km long (fig. 9), the longest active lava flow in the solar system.

Summary of Volcanism in the Solar System

Evidence of volcanism is found throughout the solar system where rocks can be seen. The most common type of lava is basalt, and various forms of evidence (rock samples, telescopic data, spectroscopic data, and so on) indicate that basalt is present throughout our inner rocky planets and some asteroids. In addition, most eruptions are primarily effusive but consist of a modest component of explosive activity because of its low viscosity of eruptive material. This is comparable to the type of activity found at S P Mountain (known locally as S P Crater) (fig. 10) in the San Francisco Volcanic Field and will be described in detail in the following sections.

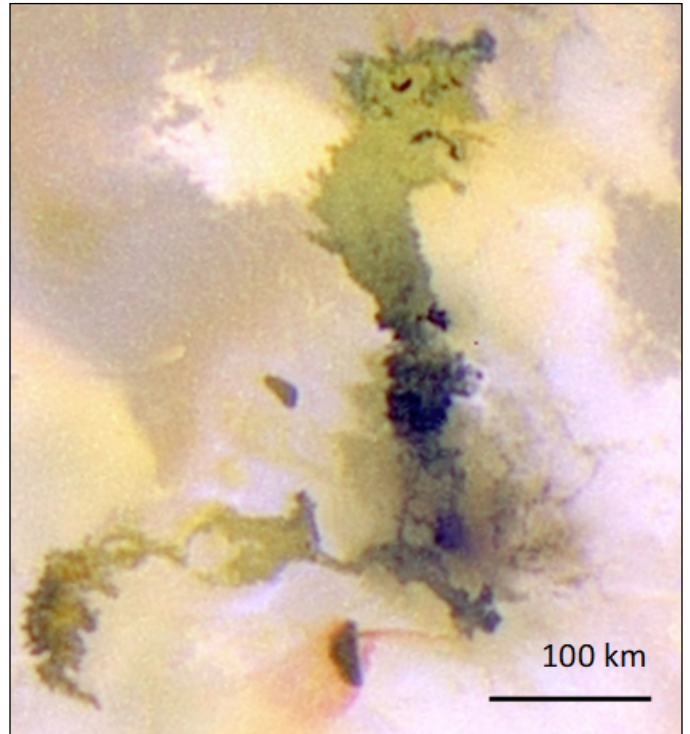


Figure 9. Satellite image of Amirani (an active volcano on Io) and its flow field (image ID PIA03533) (25.0 °N, 115.2 °W). Photograph by National Aeronautics and Space Administration (NASA), Jet Propulsion Lab (JPL), University of Arizona, and Jason Perry, University of Arizona.

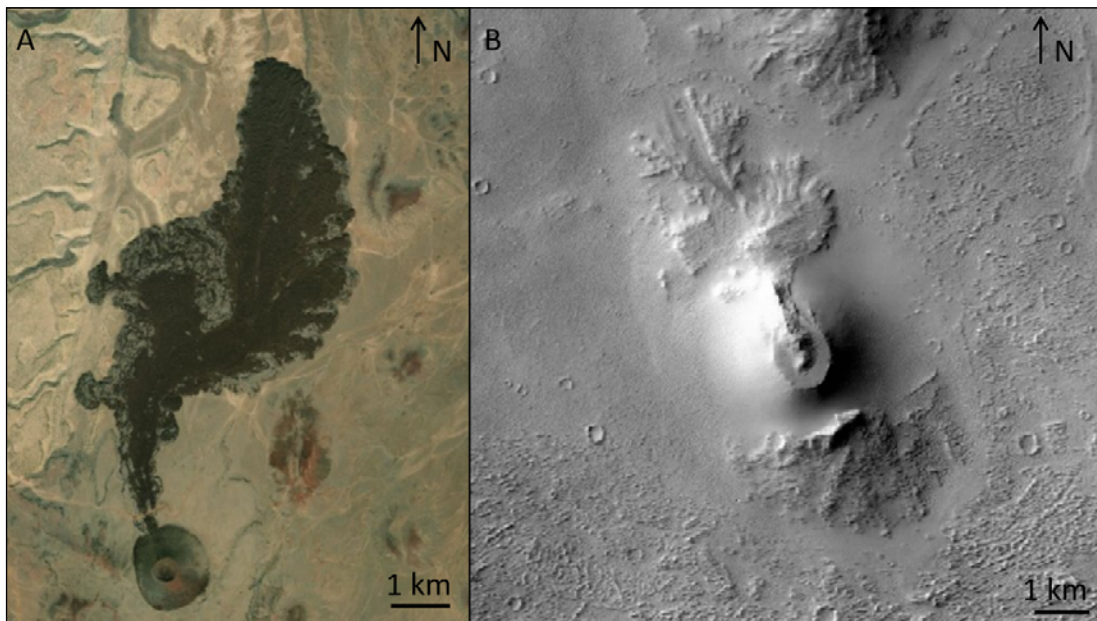


Figure 10. Satellite image comparing S P Mountain (A) to a satellite image of a volcano on Mars (B) (CTX image P22_009554_1858_XN_05N122W) (5.6 °N, 237.0 °E) of similar size. Basemap of (A) is by Esri, Maxar Technologies, GeoEye, Earthstar Geographics, CNES, Airbus DS, U.S. Department of Agriculture (USDA) Farm Service Agency, U.S. Geological Survey (USGS), AeroGRID, IGN, and the GIS User Community, data served by Esri web service (https://services.arcgis.com/ArcGIS/rest/services/World_Imagery/MapServer), Map data 2021. Image (B) is by National Aeronautics and Space Administration (NASA), Jet Propulsion Lab (JPL), Arizona State University, and Malin Space Science Systems.

A Brief Geologic History of the Colorado Plateau and San Francisco Volcanic Field

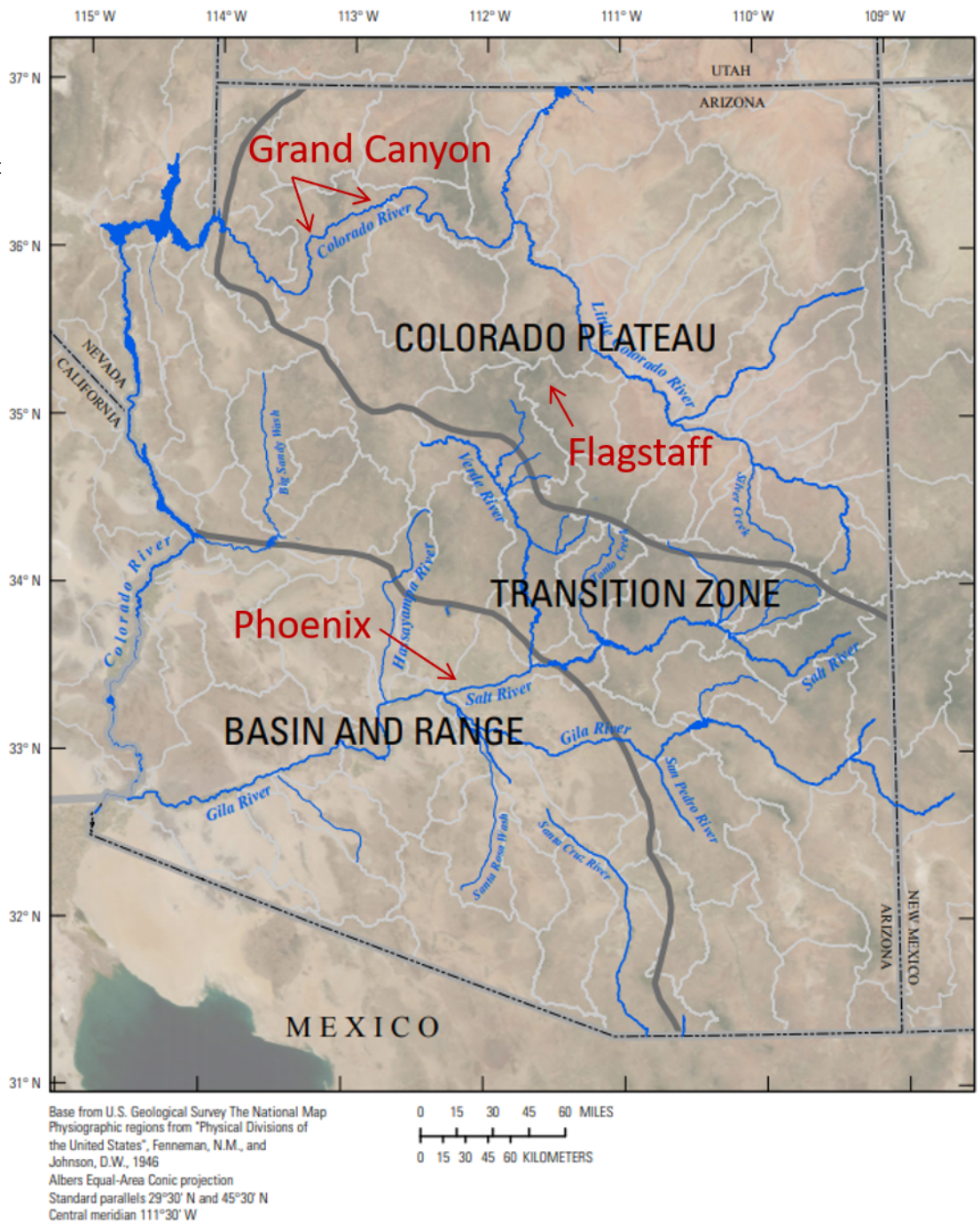
The Physiographic Provinces of Arizona

Arizona is divided into three main physiographic provinces: the Colorado Plateau, Transition Zone, and Basin and Range Provinces (fig. 11). The San Francisco Volcanic Field is located near the southwest edge of the Colorado Plateau Province. For context, the physiographic areas surrounding Flagstaff, the Grand Canyon, and Phoenix have been annotated on figure 11, a map of Arizona.

Raising the Colorado Plateau

The Colorado Plateau Province is a slab of continental crust that has an average crustal thickness of ~45 km (Zandt and others, 1995; Mooney and others, 1998), an average height of 2 km above sea level (Mooney and others, 1998), and extends across parts of Arizona, New Mexico, Colorado, and Utah (fig. 12). The Colorado Plateau Province is bounded by the Basin and Range Province from the northwest and extending down to the south and southeast and the Rocky Mountains to the east (fig. 12), all of which have experienced intense tectonic deformation. The Colorado Plateau Province, on the other hand, has remained largely undeformed and is considered to be in isostatic equilibrium (Levander and others, 2011).

Figure 11. Map of Arizona showing the three main physiographic provinces that compose Arizona (Colorado Plateau, Transition Zone, and Basin and Range) in black text (from Kennedy and others, 2015). The Grand Canyon, Flagstaff, and Phoenix (red text) are included for reference.



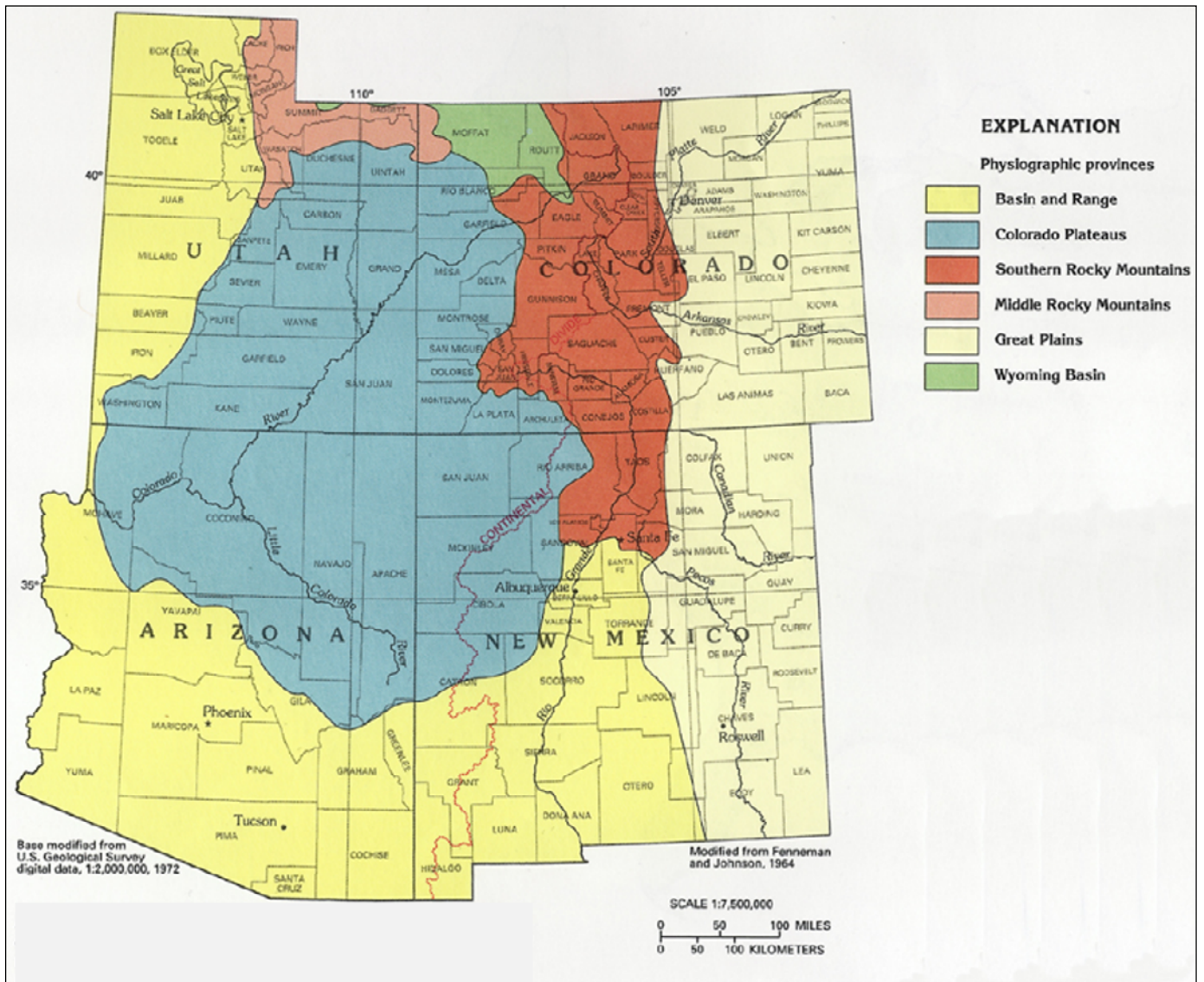


Figure 12. Map of the physiographic provinces in Utah, Colorado, Arizona, and New Mexico (Fenneman and Johnson, 1964; Robson and Banta, 1995).

The mechanisms responsible for raising such a large segment of the continental crust to over 2 km above sea level while maintaining its internal structure remain a contested topic (McQuarrie and Chase, 2000; Roberts and others, 2012, and references therein). Explanations include such processes as thickening through crustal shortening (McQuarrie and Chase, 2000; Davis and Bump, 2009), partial removal of the mantle lithosphere through low-angle subduction (Spencer, 1996) or from delamination (Zandt and others, 1995; Levander and others, 2011), and magmatic injection (Morgan and Swanberg, 1985). It is possible that a combination of some of these mechanisms are responsible for the current state of the Colorado Plateau Province. However, increasing evidence supports Colorado Plateau Province uplift driven by convective lithospheric downwelling (Karlstrom and others, 2008; Moucha and others, 2008, 2009; van Wijk and others, 2010; Crow and

others, 2011; Levander and others, 2011). Through various heat-flow and convective-numerical modeling, researchers theorize that multiple uplift events occurred in the Colorado Plateau during the Laramide orogeny (late Mesozoic through middle Cenozoic Era) (Humphreys, 1995; Huntington and others, 2010), the middle Cenozoic Era (Humphreys and others, 2003; Spencer, 1996), and late Cenozoic Era (Karlstrom and others, 2008; Moucha and others, 2009; van Wijk and others, 2010).

Rock Ages of the Colorado Plateau Province

The Colorado Plateau Province predominantly comprises sedimentary rocks formed during the Neoproterozoic, Paleozoic, and Mesozoic Eras (ranging in age from ~1.2 billion years ago [Ga] to 200 million years ago [Ma]), and are generally crystalline

10 A Geologic Field Guide to S P Mountain and its Lava Flow, San Francisco Volcanic Field, Arizona

basement rocks of Paleoproterozoic age (~1.9–1.7 Ga) (Davis and Bump, 2009). During the deposition of Colorado Plateau sedimentary rocks, crustal elevation was at or near sea level (Mooney and others, 1998; McQuarrie and Chase, 2000). Based on current crustal-thickness maps, continental crust at sea level is relatively thin, implying that the Colorado Plateau Province was also thin (estimated to be ~30 kilometers [km] thick) and subsequently increased in thickness after deposition of the sedimentary sequences (McQuarrie and Chase, 2000). The San Francisco Volcanic Field, in the southwestern Colorado Plateau Province, comprises sedimentary rocks ranging in age from Cambrian (Tapeats Sandstone, ~545 Ma) to Triassic (Moenkopi Formation, ~240 Ma) (fig. 13), the younger

volcanic rocks cover much of the area. This entire package overlies Paleoproterozoic granite and schist, which are exposed at the base of the Grand Canyon.

San Francisco Volcanic Field

Basalt of Miocene to early Pliocene age, referred to as rim basalts, border the south boundary of the Colorado Plateau Province along the Mogollon Rim and extend up to the southern boundary of the San Francisco Volcanic Field (Luedke and Smith, 1978; Tanaka and others, 1986). The San Francisco Volcanic

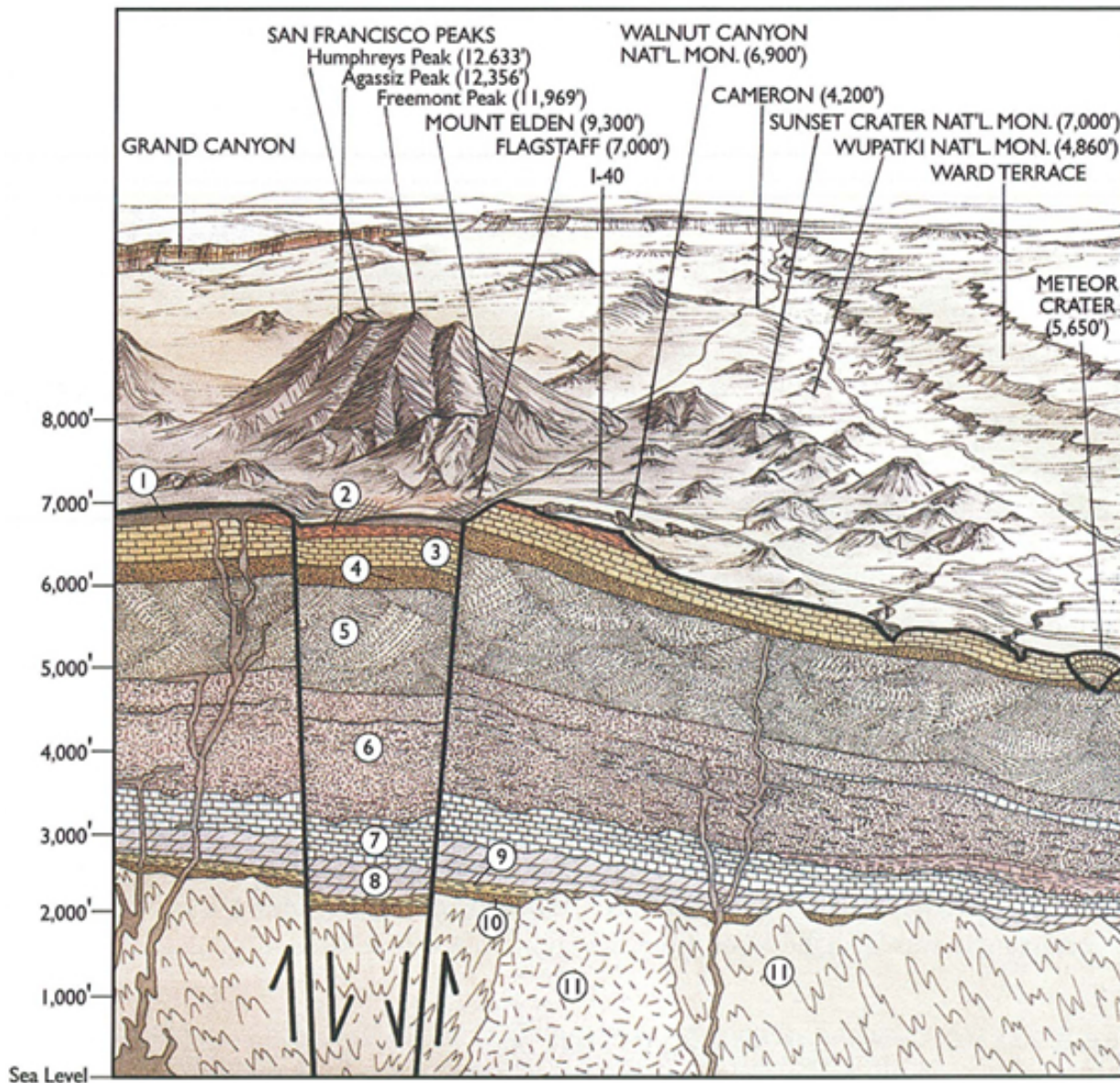


Figure 13. Geologic block diagram showing the surface and subsurface geology of the Flagstaff area. The numbers on the diagram correspond to the geologic units as follows: (1) Quaternary and Tertiary volcanic rocks, (2) Moenkopi Formation, (3) Kaibab Formation, (4) Toroweap Formation, (5) Coconino Sandstone, (6) Supai Group, (7) Redwall Limestone, (8) Martin Formation, (9) Mauv Limestone and Bright Angel Shale, (10) Tapeats Sandstone, (11) Precambrian granite and schist (modified from Billingsley and others, 1980).

Field, a relatively young (late Cenozoic) volcanic field comprises more than 600 volcanoes, ranging in composition from mafic (basaltic) to intermediate (basaltic andesite to andesite) and silicic (dacite and rhyolite), and superposes some of these rim basalts (Tanaka and others, 1986). Bill Williams Mountain (a silicic volcano) and surrounding basaltic cones are the oldest volcanic features of the San Francisco Volcanic Field and overlie rim basalts, questioning whether any time lapse occurred between the waning of the Mogollon Rim volcanism and the start of the San Francisco Volcanic Field volcanism (Tanaka and others, 1986). The entire San Francisco Volcanic Field (outlined in orange in figure 14) stretches ~70 km north-south and ~100 km east-west across the southern Colorado Plateau Province. Apart from some contemporaneous basaltic volcanism, in general the silicic and intermediate constructs (for example, Bill Williams Mountains, Sitgreaves Mountain, Kendrick Peak, San Francisco Mountain, Elden Mountain, and other smaller domes) predate many of the ~600 basaltic and basaltic-andesite vents (Tanaka and others, 1986; Riggs and Duffield, 2008). Various dating techniques, such as K-Ar radiometric dating (using for example, sanidine and plagioclase phenocrysts, and whole rock), have determined that the volcanic field decreases in age from west to east (shown along

bottom of figure 14), with the youngest volcano, Sunset Crater, having erupted ~900 years ago (Robinson, 1913; Colton, 1936; Cooley, 1962; Moore and others, 1976; Tanaka and others, 1986; Ort and others, 2002).

Fault Systems within the San Francisco Volcanic Field

The extent of the San Francisco Volcanic Field and its silicic volcanoes, as well as the youngest volcano in the area (Sunset Crater), the three major fault systems (Mesa Butte, Oak Creek Canyon, and Doney), and the northern extent of rim basalts are depicted in figures 14 and 15 (Ulrich and others, 1984; Holm, 1987; Newhall and others, 1987; Ulrich and Bailey, 1987; Wolfe and others, 1987a, b; Conway and others, 1997). Shoemaker and others (1978) postulated that these major fault systems, which trend to the northeast with downward motion to the east (Ulrich and Bailey, 1987; Conway and others, 1997) originated deep within Proterozoic basement rocks and were subsequently reactivated during the late Cenozoic. Numerous volcanic vents align with these faults, which likely influenced vent locations

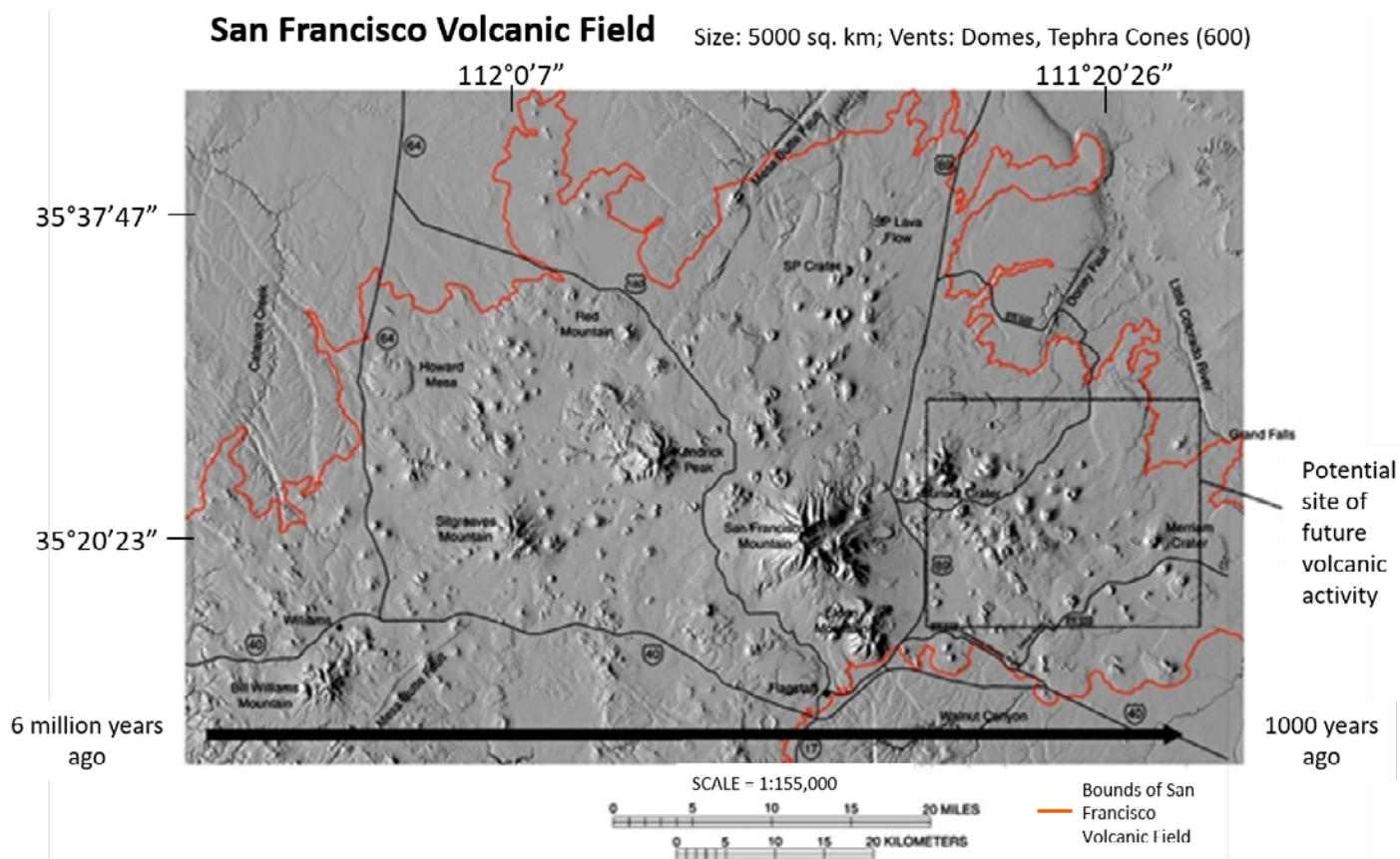


Figure 14. Digital elevation model (DEM) of the San Francisco Volcanic Field. Orange line is the boundary of the San Francisco Volcanic Field. The black arrow represents the volcanic field decreasing in age from west to east. Several major volcanic vents have been labeled, and the black box highlights the location of a future potential site for volcanic activity. S P Mountain is labeled as SP Crater. Base image provided by the National Aeronautics and Space Administration (NASA). Annotations by the Arizona Geological Survey (<https://azgs.arizona.edu/photo/san-francisco-volcanic-field-arizona>).

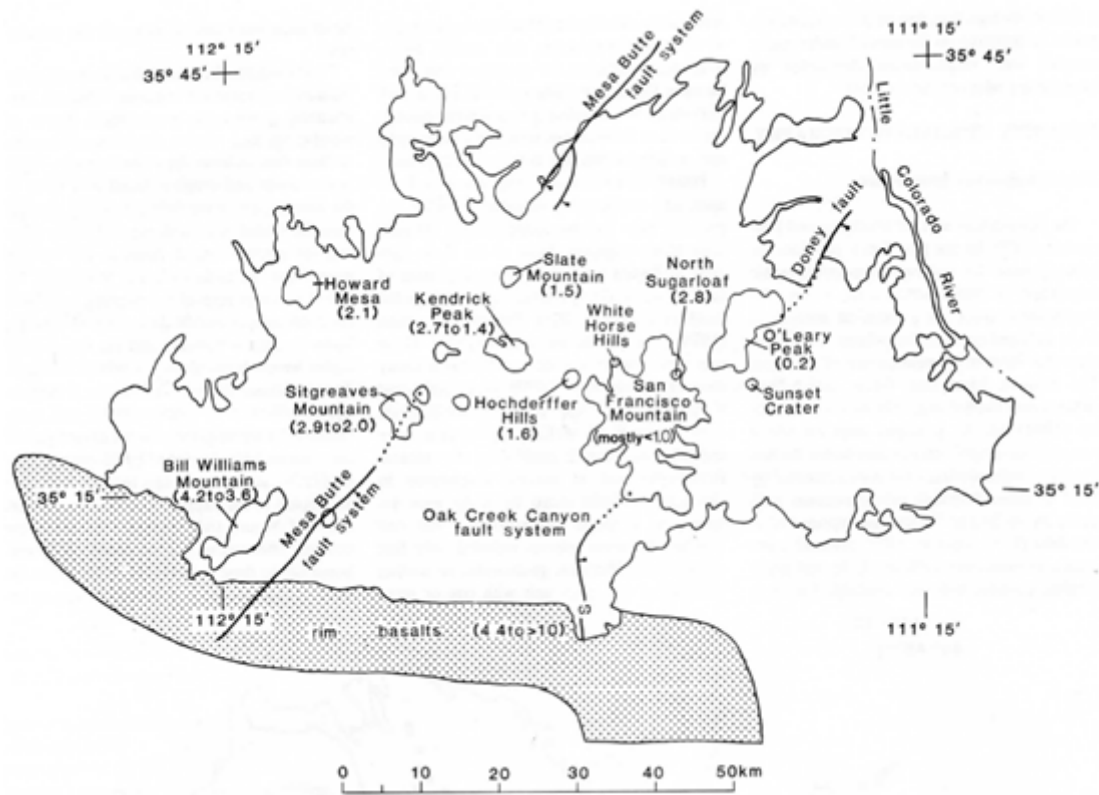


Figure 15. Illustration of the extent of the San Francisco Volcanic Field (outline of image, not including the rim basalts; same outline as in figure 14, shown in orange) and its silicic and intermediate vents, major fault systems, and the northern extent of rim basalts. Numbers in parentheses are estimated ages in millions of years derived from K-Ar dating (using whole rock and individual phenocrysts, such as plagioclase and sanidine) (Tanaka and others 1986).

and allowed easier passage for magma to ascend to the surface. For example, Sitgreaves Mountain, Kendrick Peak, and Slate Mountain (all silicic vents) and Red Mountain cinder cone are situated along the ~150 km long Mesa Butte fault system, and the Oak Creek Canyon fault lies directly beneath San Francisco Mountain (Shoemaker and others, 1978; Ulrich and Bailey, 1987; Conway and others, 1997).

Sources of Volcanic Rock Compositions

The San Francisco Volcanic Field is a unique volcanic field because it includes a diverse and complete continuum of volcanic rocks, ranging from basalt to rhyolite in composition. The likely petrogenetic origins for the range of volcanic rock types that are found in the San Francisco Volcanic Field are (group 1) basaltic magmas of various compositions sourced from both the lithospheric and asthenospheric mantle; (group 2) crystal fractionation of these mafic magmas; (group 3) crustal melting, which resulted in the formation of an evolved silicic melt; or (group 4) the mixing of melts from either group 1 (basaltic in composition) or group 2 (an intermediate compositional melt)

with the evolved silicic melt generated in group 3 (Bloomfield and Arculus, 1989; Arculus and Gust, 1995; Chen and Arculus, 1995; Reid and others, 2012).

To review the full range of volcanic rock types of the San Francisco Volcanic Field, refer to Moore and Wolfe (1987), Newhall and others (1987), Ulrich and Bailey (1987), and Wolfe and others (1987a, b).

Distributed Volcanism and Associated Volcanic Features

Distributed Volcanic Fields and Clusters

Typical distributed volcanic fields comprise numerous volcanic vents that are close together in space and time. Distributed volcanism is common on both Earth and Venus, though remnants of this type of volcanic distribution have also been observed on the Moon and possibly Mars (Campbell and others, 2009; Brož and Hauber, 2012). Vents within large volcanic

fields (for example, San Francisco Volcanic Field) tend to form in clusters (Connor and others, 1992; Conway and others, 1998). For example, S P Mountain is part of the S P cluster, which comprises 62 tephra cones, tuff rings, and spatter cones (Ulrich and Bailey, 1987; Conway and others, 1997) and spans an area of ~350 square kilometers (km²) (Conway and others, 1998). A combination of radiometric and surface-exposure dating, geomorphology, volcanic stratigraphy, and paleomagnetic data were used to acquire vent ages (Ulrich and Bailey, 1987; Mullaney, 1996; Conway and others, 1997; Tanaka and others, 1991; Fenton and Niedermann, 2014). The oldest basaltic flow in the vicinity of S P Mountain is the Cedar Ranch mesa flow, which formed ~5.6 Ma (Ulrich and Bailey, 1987). Volcanic activity within this area is estimated to have lasted until ~16,000 years ago (~16 ka), most vents having formed less than 780 ka (Conway and others, 1998).

Eruption Styles

One of the main driving forces behind a volcanic eruption is the expansion of volatiles; elements or compounds, like H₂O and CO₂, form a gas at relatively low pressure but are dissolved in magmas at depth (Wilson and Head, 1981). These volatiles will exsolve from the magma and coalesce as the magma ascends from depth in a conduit and decompression occurs. Depending

on ascent rate and the extent to which gas bubbles grow and coalesce to form gas-rich pockets, the eruption can be dominated by sporadic explosions or by continuous fountaining. The style of eruption dominated by moderate to high fountains is called Hawaiian, and highly vesicular lapilli-sized tephra are the most common eruptive product. The more sporadic style of eruption is called Strombolian and usually produces less vesicular and larger sized tephra. In both cases, the lava that is expelled into the atmosphere usually cools very quickly, followed by varying degrees of fragmentation. The rapid cooling inhibits the growth of larger crystals and often quenches the liquid lava into a glass. However, in some circumstances, the column of erupting lava is so dense and energetic that the lava fragments are still fluid when they land, forming spatter. If the spatter deposit builds quickly, it can retain sufficient heat for the clasts to weld together and form agglutinates, a welded pyroclastic deposit. In the extreme case, the spatter deposit can be thick and fluid enough to remobilize and flow as a rheomorphic lava flow. More commonly, the tephra deposits fall to the ground as solid particles that, over time, build an edifice around the vent. If the vent is focused around a single point, a cone like S P Mountain is built. If the vent is a fissure, the cone that will form will be more elongated; for example, the volcanic feature to the northeast of S P Mountain (fig. 16) is an elongated cone.



Figure 16. Satellite image of the field site includes S P Mountain, a structural graben, an elongated cone, and Colton Crater. White boxes show locations of subsequent images and photographs. The numbers indicate the corresponding figures. Image is by Esri, Maxar, GeoEye, Earthstar Geographics, CNES and Airbus DS, U.S. Department of Agriculture (USDA), U.S. Geological Survey (USGS), AeroGrid, IGN, and the GIS User community.

Lava Flows

Another common feature associated with volcanic fields are lava flows. In the San Francisco Volcanic Field, lava flows are usually sourced by small vents near the base of tephra cones, though some flow directly from the summit vent (Valentine and Connor, 2015). Lava flows can occur concurrently with Strombolian and (or) Hawaiian eruptions, during which tephra will often fall onto and coat the upper surface of the lava flow or after the cone building stages have ended (in other words, tephra will not blanket the lava flow at this stage). S P Mountain is a classic example of a tephra cone and its co-eruptive lava flow.

S P Mountain and its Lava Flow

The Age of S P Mountain

S P Mountain is a tephra cone that formed during a single eruptive period, though the age of the eruption is still uncertain. Surface-exposure dates using ^3He and ^{21}Ne (Fenton and Niedermann, 2014) and whole rock K-Ar radiometric dating (Baski, 1974) have yielded a similar eruption age of ~ 70 ka. However, based on the well-preserved morphology of S P Mountain compared to other cones in the San Francisco Volcanic Field, many researchers suggest this age is too old. Rittenour and others (2012) used an additional technique for dating S P Mountain, optically stimulated luminescence (OSL) of quartz xenocrysts within the flow. This method estimated

an eruption age of $\sim 6\text{--}5.5$ ka, which is better aligned with the geomorphic character of S P Mountain and its lava flow (Rittenour and others, 2012).

Dimensions of S P Mountain and General Features

The volcanic cone is 250 meters (m) (820 feet [ft]) tall and its base is $\sim 1,200$ m (3,900 ft) in diameter (fig. 17) and is situated on the lower flanks of a preexisting volcano located to the west. The summit crater is 400 m (1,300 ft) in diameter and ~ 120 m (400 ft) deep (Ulrich and Bailey, 1987). Both the block lava flow that extruded from the cone's base as well as the cone itself are basaltic andesite in composition, and both were sourced from the central vent (Ulrich and Bailey, 1987). The S P Mountain lava flow extends to the north and covers older flows that erupted from other local vents.

Dimensions of S P Mountain Lava Flow and General Features

S P Mountain's blocky lava flow is texturally different from the most common types of basaltic lava morphologies, that is, pāhoehoe and 'a'ā. Pāhoehoe lava flows display a smooth, often ropy-like surface, whereas 'a'ā flows are rough, sharp, and have a rubbly surface. Block lava flows, on the other hand, tend to be more viscous, resulting in the lava cooling and fragmenting into large polygonal blocks.

S P Mountain's blocky lava flow is 7.0 km (4.3 miles) long. Nearest to the cone, the flow is 250 m (820 ft) wide and

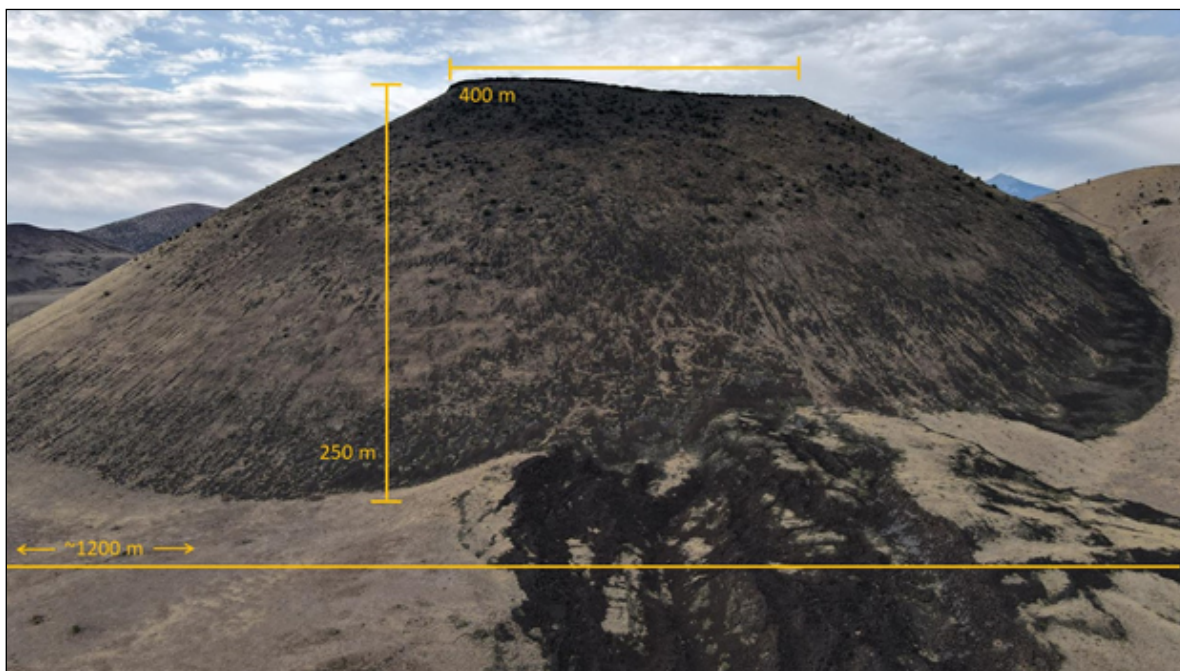


Figure 17. Photograph of an oblique view of S P Mountain (view to the south), showing the volcano's dimensions. S P Mountain is 250 meters (m) tall; its summit crater is 400 m in diameter, and its base is $\sim 1,200$ m in diameter. Photograph by M. Elise Rumpf, U.S. Geological Survey.

15 m (50 ft) thick and spreads out to 3.9 km (2.4 miles) at its widest and 55 m (180 ft) thick at its distal end (Ulrich and Bailey, 1987). This flow displays two distinct surface textures that can be observed both on the ground and aerially (fig. 18) and will be referred to as surface texture 1 and 2 herein. Surface texture 1 has several distinct characteristics that include

transported mounds of agglutinated near-vent material found along the flow surface, a thin coating of both tephra and soil, and coverage by low grassy vegetation (Schaber and others, 1980). Surface texture 2 displays a much blockier texture and lacks all the previously described characteristics associated with surface texture 1.

Figure 18. Photographs of lava flow near S P Mountain showing the contrast between surface texture 1 and 2. *A*, Lava flow proximal to the base of S P Mountain (S P Mountain is located just out of the image, to the south). Arrows point to a lava levee. *B*, Oblique view of the lava flow. Surface texture 1 is coated by a thin layer of tephra and soil, is vegetated, and has transported mounds of the agglutinated material within the flow. Surface texture 2 lacks tephra and soil coverage, is much blockier, and has minimal vegetation growth. Photograph A is by Esri, Maxar, GeoEye, Earthstar Geographics, CNES and Airbus DS, USDA, USGS, AeroGRID, IGN, and the GIS User Community. Photograph B is by M. Elise Rumpf, U.S. Geological Survey.



Lava Flow Emplacement Theories

There is some uncertainty as to whether S P Mountain lava flow consists of one flow (theory 1) or two separate but stacked flows that were emplaced at different stages during the eruption (theory 2). Theory 1 describes the different textures to be the result of varying degrees of cooling (Hodges, 1962; Schaber and others, 1980). Hodges (1962) described surface texture 1 to be red basalts that appear highly weathered. These basalts are typically found along the margins of the flow and are always associated with soil accumulation and vegetation. Hodges (1962) postulated that as the lava flow extruded from the vent, the margins of the flow cooled much faster than its insulated interior. Therefore, the rapidly cooled margins have a higher glass content compared to the flow interior and can alter more readily. In addition, Hodges (1962) speculated that the margins have an increased concentration of gases during eruption, which can result in a higher oxidation to the basalt flow. The combination of oxidation and high glass content thus causes this portion of the flow to be weathered at a higher rate and therefore has increased soil accumulation. Hodges (1962) described surface texture 2 as being a typical block flow, characterized by its equidimensional-polygonal blocks that formed when the lava cooled and contracted.

Roughly 4.5 km downstream from where the lava extruded from the vent is an outcrop of altered red basalt that extends from the margins of the flow to its interior (fig. 19). Hodges (1962) suggested that the now altered red basalt was part of an initial lava flow eruption phase that began to cool and solidify. A subsequent, secondary pulse of lava was obstructed by the initial, now-cooled lava and was forced to divert to the east.

Theory 2 describes the S P Mountain lava flow as comprising two separate, stacked flows. The theory delineates the older flow (surface texture 1) to be the vegetated, soil- and tephra-covered flow that is exposed along the margins (Sabels, 1960; Weikart and others, 2008; Rittenour and others, 2012). The younger lava flow (surface texture 2) is absent of tephra and soil coverage, lacks vegetation, and is much blockier. Weikart and others (2008) suggest the older lava flow erupted concurrently with the Strombolian eruptions responsible for building the cone of S P Mountain. This initial lava flow was destructive, in which agglutinated material from the cone was ripped off and transported downstream. As the mass flux for the lava flow decreased, Strombolian activity continued and rebuilt the cone. The final lava flow erupted after the cone-building phase had ceased and was not destructive to the cone, indicated by a lack of tephra coverage and agglutinated cone material on the flow, respectively.

S P Graben

Along the western margins of the S P Mountain lava flow, the flow spilled into a graben at two separate locations (fig. 20). Named S P graben by Babenroth and Strahler (1945), this graben trends to the north, is ~13 km (8 miles) long and ~400 m (0.25 miles) wide. The graben walls are asymmetric, the western wall stands ~60 m (200 ft) tall and the eastern wall extends ~14 m (45 ft) above the graben floor (Babenroth and Strahler, 1945). The graben is exposed in Kaibab Limestone, though its floor has been covered by younger lava flows and sediment.

Figure 19. Photograph of an agglutinated mound that was transported away from the vent downstream. This mound is near the spillover, closer to S P Mountain, into the graben. Photograph by Amber Gullikson and M. Elise Rumpf, U.S. Geological Survey.



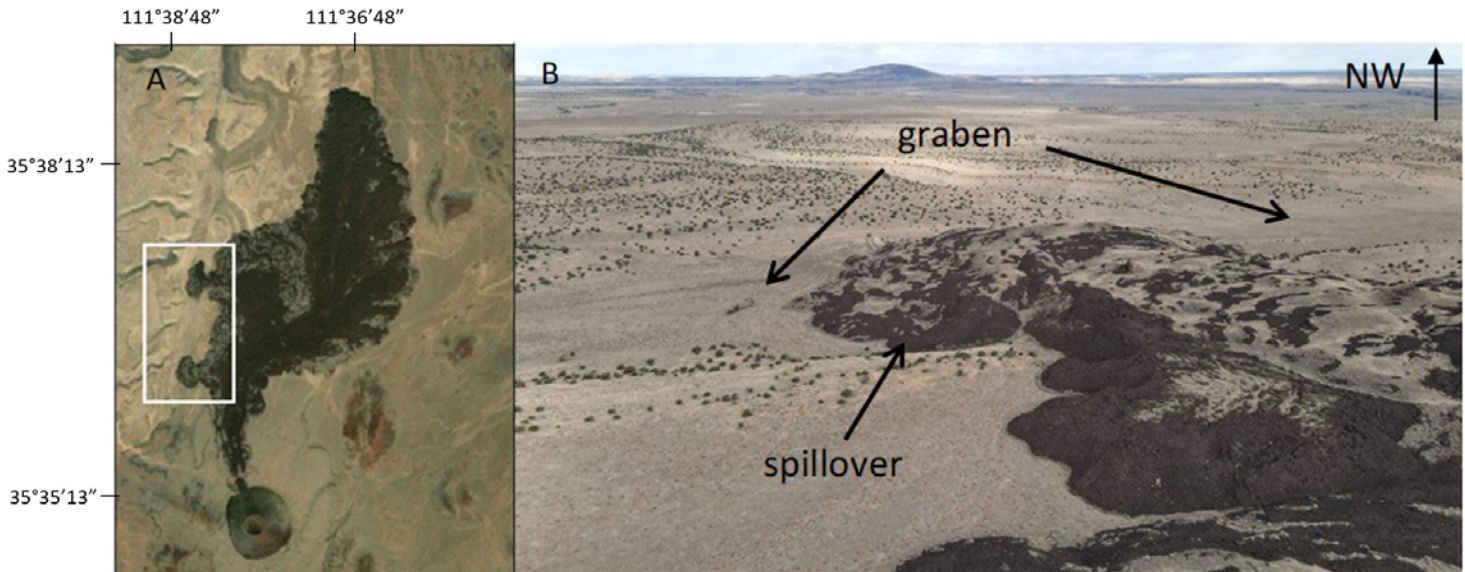


Figure 20. Photographs of the S P Mountain lava flow showing the graben and spillovers. *A*, Satellite view of the two lava spillovers into the graben (highlighted by a white box). *B*, An oblique view of the spillover nearest to the vent. Photograph A is by of Esri, Maxar, GeoEye, Earthstar Geographics, CNES and Airbus DS, USDA, USGS, AeroGRID, IGN, and the GIS User Community. Photograph B is by M. Elise Rumpf, U.S. Geological Survey.

Getting to S P Mountain

Take U.S. Highway 89 north from Flagstaff. Once Highway 89 diverts from both Interstate 40 and Historic Route 66, travel an additional 29.4 miles on Highway 89. Once past the turnoff for the Wupatki National Monument (on the east side of the road), the turnoff onto the unmarked dirt road will be 3.0 miles farther north on the left. Turn left (west) onto the

dirt road and drive for 7 miles. At mile 3.2, the road will begin to veer south and parallel to the S P Mountain lava flow.

When both the lava flow and tephra cone come into view, review figure 21 to determine what type of morphologic features can be identified. Observe the location of the source of the lava flow (that is, the contact between the lava flow and the tephra cone), the lava flow itself, possible transported mounds, crater rim, fallout-dominated beds, and the debris apron. Numerous degraded cones are visible to the north and south as you drive along this road.

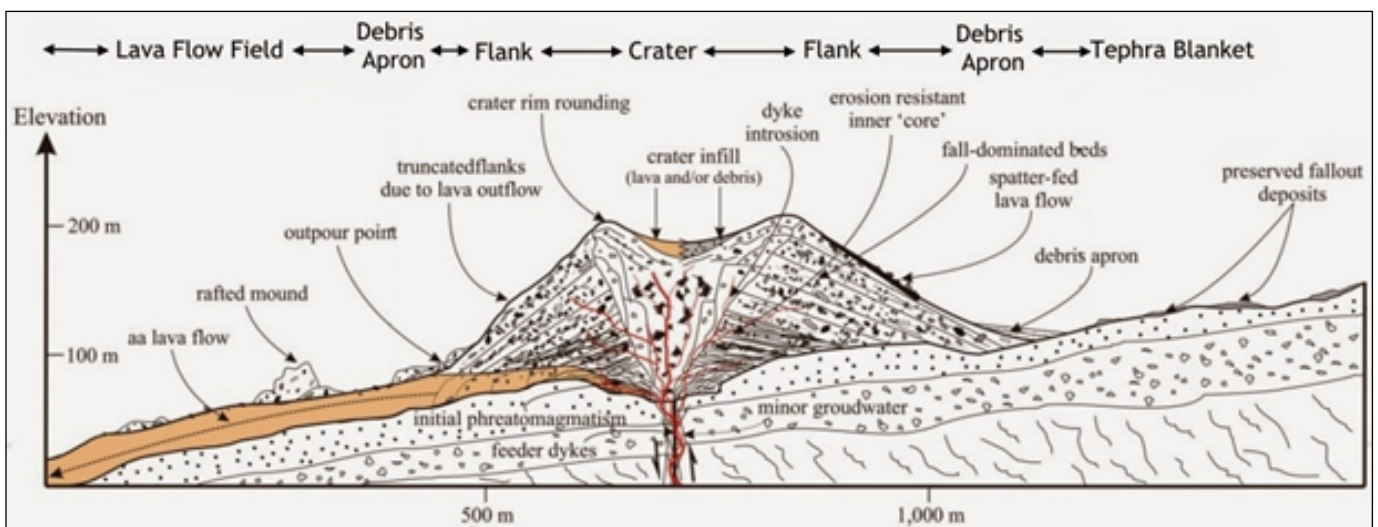


Figure 21. Schematic cross section of a typical tephra cone. Depicted in this illustration are both volcanic sedimentary processes and geomorphic structures. Illustration from Kereszturi and Nemeth (2012).

At mile 7, the road crosses over the S P Mountain lava flow. Drive over the lava flow and park on the left (south) side of the road. A disused road traverses up the saddle; turnoff and park near this old road (lat 35°35'20.34" N., long 111°38'14.7" W.) (fig. 22).

Disclaimer

S P Mountain is located on private property, owned by the Babbitt family. The Babbitts generously allow public use of their land, though it is expected that wildlife and cattle are not disturbed, and artifacts and rocks are left in place. Please refrain from smoking or having open flames of any kind while on the land. If you plan to do any sampling, operate drones, or use other instrumentation, please contact the Babbitts at <https://www.babbitt ranches.com/contact-us>.

In addition, hiking up S P Mountain can be very strenuous. You will encounter loose rocks and cacti. Do not try to hike S P Mountain if you do not have plenty of water and are not wearing appropriate clothing and shoes. During the summer months temperatures can be high, especially when hiking on basalt, so please plan accordingly.

Stop 1. Source of the Lava Flow

Walk back east along the road until you reach the lava flow, then turn south, and hike along the flow until you near the base of S P Mountain. This stop is located near the contact between the lava flow and the tephra cone (fig. 22).

Goal.—Describe the types of tephra observed at this location.

Need to know.—This is the location where the lava flow extrudes from the base of the cone (outpour point in figure 21). As lava flows out from this point, portions of the cone can be ripped away and transported by the lava flow. Such transported mounds of the cone will be observed at the lava flow and graben stops (stop 3 and 5, respectively).

A few tens of meters from the contact (and more pronounced at the lava flow stop [stop 3]) are levees. Lava flow levees form from cooled lava at the edge of active lava flows. They build higher with periodic flux increases that cause lava to spill out of the channel. As the flux of lava in the channel wanes at the end of an effusion event, the interior of the channel drains and leaves high standing levees, which record the maximum height of the flow (figs. 23 and 24).



Figure 22. Satellite image of S P Mountain, highlighting the locations of the first four stops of the field guide. The circle shows the location where cars should park for these stops. The white dashed line shows the preferred hiking path to stop 4, the rim. Image is by Esri, Maxar, GeoEye, Earthstar Geographics, CNES and Airbus DS, U.S. Department of Agriculture (USDA), U.S. Geological Survey (USGS), AeroGrid, IGN, and the GIS User community.

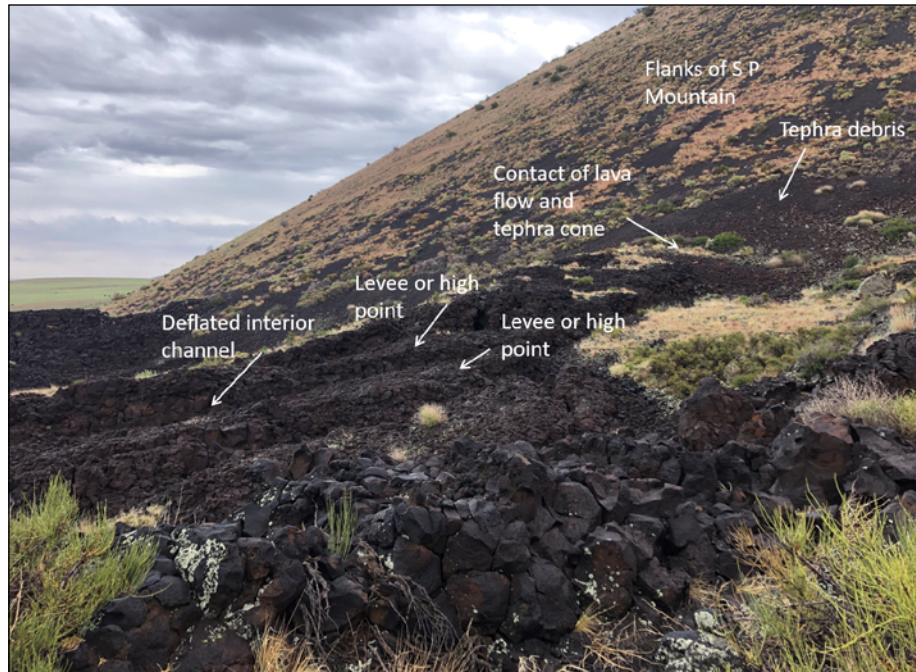


Figure 23. Photograph of the source of the lava from stop 1. Looking to the southeast, the flanks of S P Mountain are in the upper right and the lava flow is in the lower half of the image. Arrows point to the contact between the lava flow and tephra cone, tephra debris, deflated interior channel, and the location of levees on the outer edges of a lava channel. Global positioning system (GPS) coordinates, lat 35°35'16.7" N, long 111°38'05.7" W. Photograph by Amber Gullikson and M. Elise Rumpf, U.S. Geological Survey.

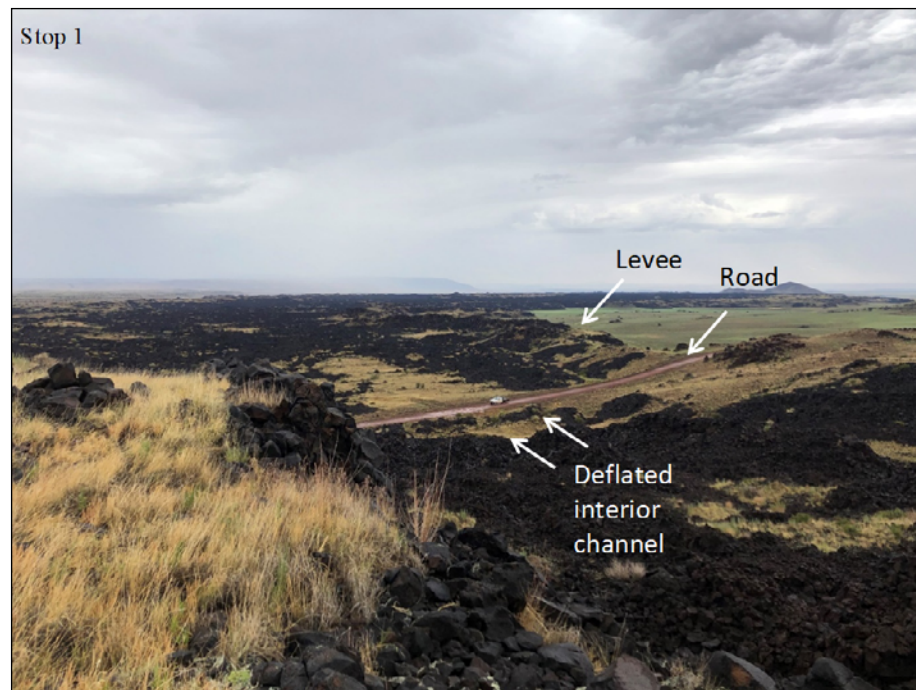


Figure 24. Photograph looking north from stop 1. S P Mountain is located behind this image, and the flow extends to the north. Arrows point to the deflated interior channel, one of the outer levees, and the road that cuts through the lava flow. Global positioning system (GPS) coordinates, lat 35°35'16.7" N., long 111°38'05.7" W. Photograph by Amber Gullikson and M. Elise Rumpf, U.S. Geological Survey.

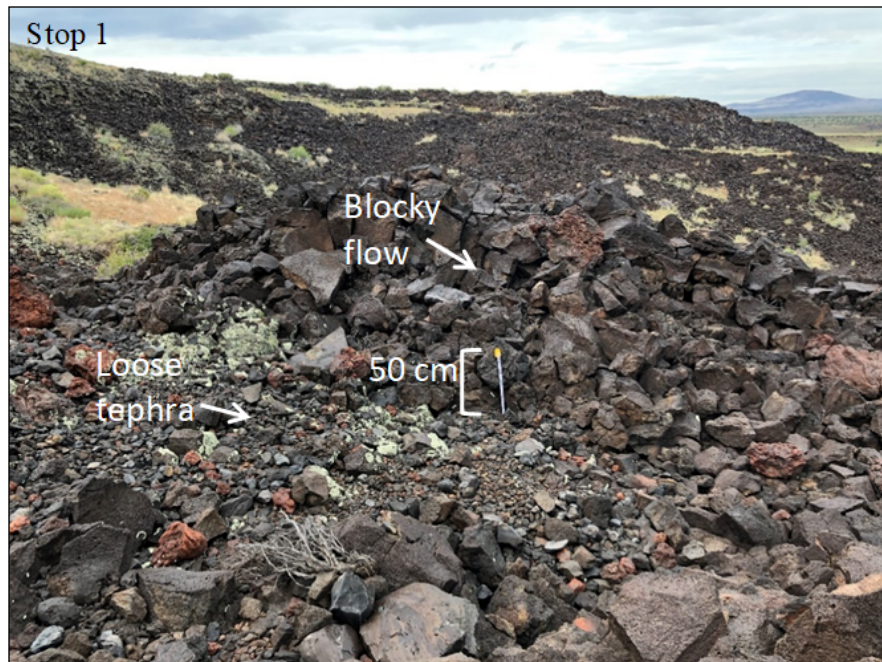


Figure 25. Photograph looking west from stop 1. The flanks of S P Mountain are to the left of the image, and the lava flow extends out to the right. Loose tephra noted on the left side of the image are erosional debris from the upper flanks of S P Mountain, deposited on top of the blocky lava flow. Global positioning system (GPS) coordinates, lat 35°35'15.0" N., long 111°38'02.0" W. Photograph by Amber Gullikson and M. Elise Rumpf, U.S. Geological Survey.

The exact location of the contact between the lava flow and tephra cone is concealed by loose tephra (fig. 25). Two major size classifications for tephra are identified here: lapilli and lava bombs (fig. 26 and table 3).

Task.—Describe the types of tephra that you observe at this location. Include color, vesicularity, size, and any other additional textures that you observe. If more than one type of tephra is observed here, estimate the population ratio between the different types and their size distributions. Is one type more prevalent than another?

Summary.—Shown in figures 27 and 28 are the two main types of tephra observed at this location. Type 1 tephra is black and dark gray in color, blocky in shape, and poorly to highly vesicular (some vesicles are elongated). Large blocks of this type commonly display submeter thick bands of varying color and vesicularity, which are likely expressions of individual tephra fragments (fig. 29A). The elongated vesicles are indicative of still partially molten (semifluid) lava fragments that were either stretched or compressed, leaving elongated

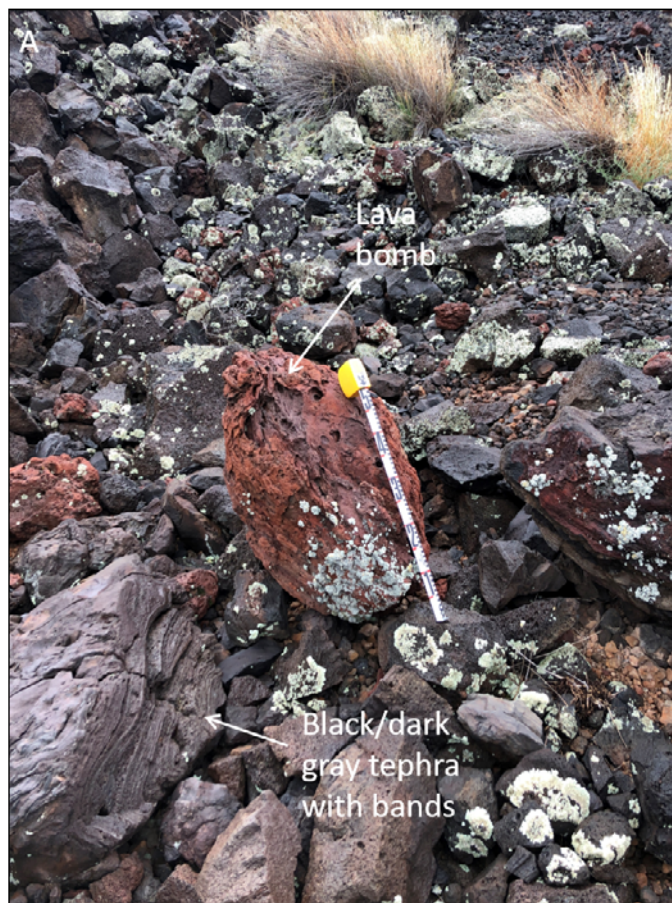


Figure 26. Photographs of a lava bomb at stop 1. Both images (A and B) are of the same lava bomb at different viewing angles. The bomb is ~60 centimeters (cm) in length and displays a typical aerodynamic oblate spheroid shape. Gray tephra with bands are located to the lower left of the lava bomb and can be seen in (A). The measuring tape is 50 cm in length. Photographs by Amber Gullikson and M. Elise Rumpf, U.S. Geological Survey.



Figure 27. Photograph looking north toward the lava flow at stop 1, S P Mountain is behind the image. Arrows point to the two different types of tephra. Note the decrease in number of red tephra farther to the north (in other words, away from the flanks of S P Mountain). Global positioning system (GPS) coordinates, lat 35°35'14.6" N., long 111°38'03.1" W. Photograph by Amber Gullikson and M. Elise Rumpf, U.S. Geological Survey.

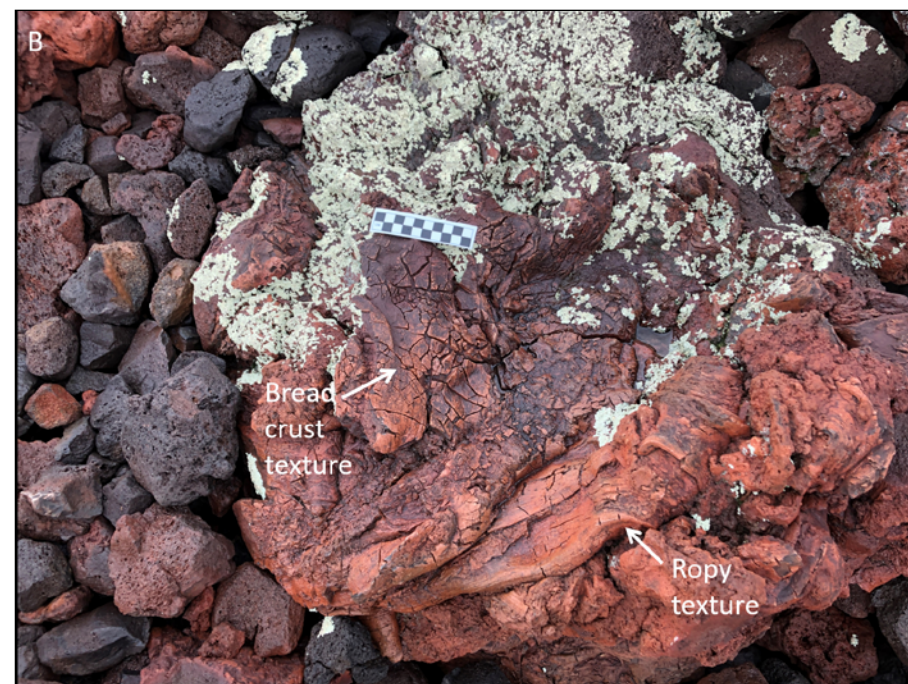
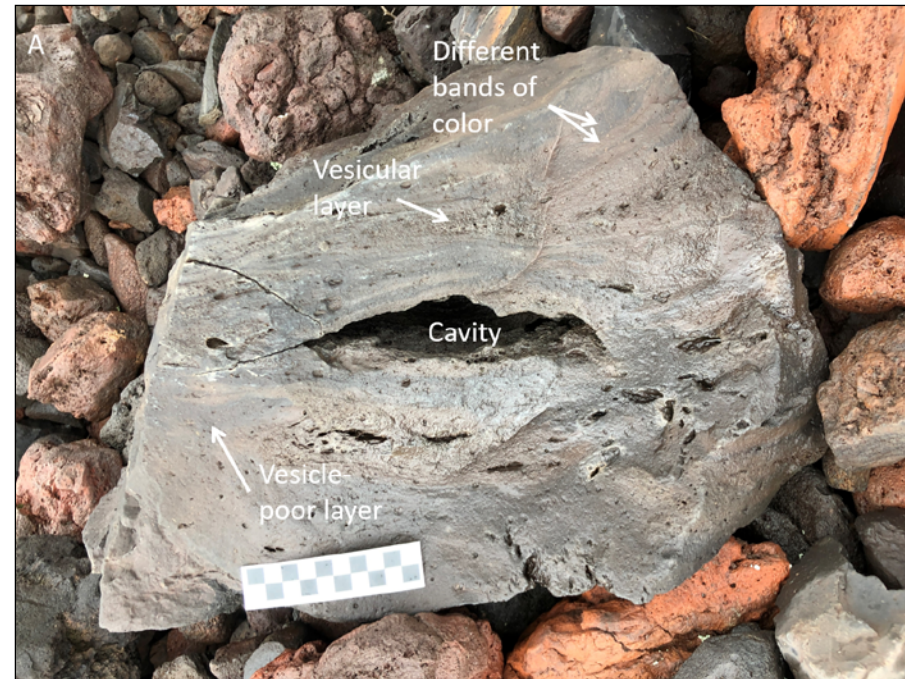


Figure 28. Photograph of the lava flow and onlapping tephra at stop 1. Arrows point to the lava flow and the onlapping tephra. Both types of tephra (such as black and dark gray tephra and red tephra) are present in this image. Global positioning system (GPS) coordinates, lat 35°35'14.7" N., long 111°38'03.0" W. Photograph by Amber Gullikson and M. Elise Rumpf, U.S. Geological Survey.

gas bubbles that were frozen in place when the lava cooled and hardened. Banding can also be discerned within this tephra type that may suggest the lava has some heterogeneities. For example, color differences between bands will typically indicate varying degrees of oxidation or glass content, though laboratory analysis

is needed to identify these subtleties. Differences in exsolved gas content is indicated by bands of varying degrees of vesicularity.

Type 2 tephra is red in color, caused by an increase in oxidation. Some tephra larger than 64 millimeters (in other words, bombs) appear welded, with a smaller subpopulation displaying both ropy and breadcrust textures (fig. 29B) and are poorly to moderately vesicular.



Agglutinated, or welded, tephra blocks are common within both types of tephra. They form when deposits of erupted lava bombs and larger lapilli fuse while still hot and plastic, or semifluid. During explosive eruptions, larger and denser fragments of lava will fall closer to the vent than smaller and less dense fragments. These larger fragments also retain heat more efficiently than smaller fragments. During Hawaiian and Strombolian eruptions, deposits of these hot and viscous fragments will accumulate proximal to vents. As material accumulates, the deposits weld together or agglutinate, owing to both the retained heat and the overpressure of the continually deposited material.

The breadcrust texture that we see on the exterior skin of some tephra is formed when the exposed surface of an erupted lava bomb cools and solidifies while the interior remains partially molten. Volatiles within the interior lava continue to exsolve, exerting an expansive force on the outer layer that causes the exterior skin to fracture (Shand, 1943; Hodges, 1962). When an elongated lava fragment is ejected and does not become rounded and aerodynamic in shape as it is hurtled through the air, it can result in a ropy or ribbon-like texture. Tephra shown in figure 29B has both the breadcrust and ropy textures. These textured portions likely formed as separate fragments, were subsequently deposited at the same location, and became welded together.

Both types of tephra drastically diminish as you move away from the flanks of S P Mountain (fig. 27).

Figure 29. Photographs of two types of tephra at stop 1. *A*, Photograph showing type 1 tephra. These tephra are black and dark gray in color, blocky in shape; elongated vesicles are observed within tephra. *B*, Photograph showing type 2 tephra. These tephra are oxidized, red in color; some appear agglutinated. Some display both breadcrust and ropy textures. The black and white checkered strip is 10 centimeters in length. Photographs by Amber Gullikson and M. Elise Rumpf, U.S. Geological Survey.

Stop 2. At the Intersection of the Road and Lava Flow

Standing on the road looking south at S P Mountain (figs. 22 and 30), you are nearly level with the outpour location of the lava flow, and levees stand at high relief on both sides of the deflated interior channel. At this location, several features from stop 1 as well as a few new additional features can be observed from different perspectives and angles.

Goal 1.—Determine the relative ages of S P Mountain and the older tephra cone directly west of it.

Goal 2.—Establish methods for measuring different features of the lava flow.

Task 1.—Along the west edge of S P Mountain is the contact between it and another tephra cone. Which of the two tephra cones is younger? How can you determine this morphologically?

Task 2.—At this stop (fig. 22), you can estimate the thickness of the flow nearest to the cone by comparing the elevation of the deflated interior channel to the surrounding terrain. To determine the difference, a global positioning system (GPS) or a high-resolution digital elevation model (DEM) are useful. If you were required to measure the height of the levees and the width of the lava flow while out in the field, how would you go about doing this? Will your methods change if you were doing this work virtually? How so?

Task 3.—Being able to model the movement of lava flows is difficult because lava is a complex fluid containing solid crystals, molten rock, and gas bubbles that change properties as it cools. What are some of the controls that affect the length and width of a lava flow? How would you go about measuring yield strength (minimum stress or force that needs to be applied to a fluid to make it move) in the field? Which parameters (for example, size, shape of the flow, and thickness) are the most difficult to measure in photographs of lava flows on other planets?

Summary.—The S P Mountain eruption that resulted in a cone and lava flow began by lava erupting along a fissure located on or near the flanks of the older tephra cone directly west. S P Mountain now partially superposes the easternmost part of the older cone. Loose tephra from the slopes of S P Mountain have eroded over time and deposited around its base and onto the older tephra cone, forming a debris apron (fig. 31). This debris apron comprises tephra ranging from submeter to a few meters in size.

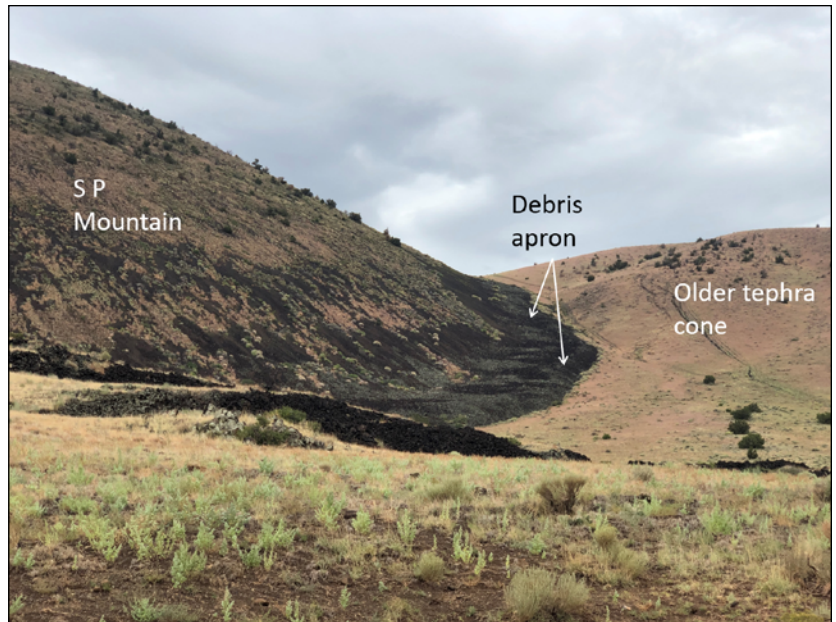


Figure 30. Photograph looking south at the contact point between S P Mountain and an older tephra cone to the west at stop 2. Tephra eroding down from the flanks of S P Mountain are forming a debris apron at the base of the cone and onto the lower flanks of the older, more degraded cone to the west. Photograph by Amber Gullikson and M. Elise Rumpf, U.S. Geological Survey.

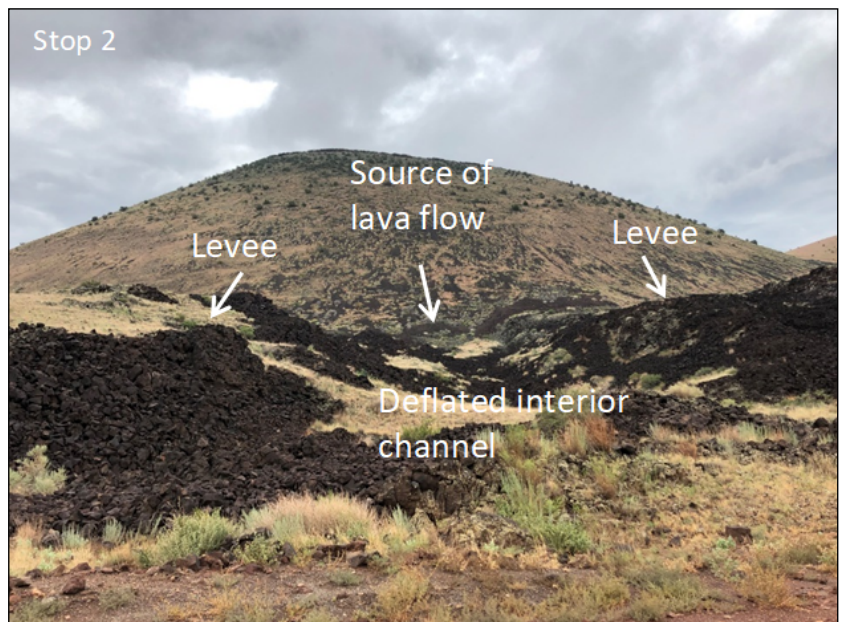


Figure 31. Looking south at S P Mountain and the source of the lava flow standing on the road near stop 2. Make note of how high the levees are compared to the deflated interior channel. Global positioning system (GPS) coordinates, lat 35°35'24.3" N., long 111°38'02.9" W. Photograph by Amber Gullikson and M. Elise Rumpf, U.S. Geological Survey.

Having a topographic map, GPS, or high-resolution DEM provides you with the necessary information to obtain measurements of the lava flow. These tools enable you to determine the elevation of each feature (such as highest point of the levees, the lowest point of the deflated interior channel, and the elevation of the surrounding terrain) to make the appropriate calculations. In addition, whether you are mapping the lava flow in the field or using satellite data, knowing the scale of your map and the outer bounds of the flow will allow you to measure the width of the lava flow along its length.

The nature of a lava flow and its movement are often complicated by factors such as crystallinity content, volatiles, and temperature; therefore, most lava flows are not considered a simple liquid. For actively flowing lava, some useful results can be obtained by assuming that the lava is a simple Newtonian fluid whose rheology can be described by a single parameter—viscosity. However, such models cannot explain why lava stops flowing. To overcome this issue, studies have used a Bingham rheology for lava, which includes a yield strength and viscosity. Using a Bingham model, lava flows stop when they become too thin for their weight to overcome the yield strength. One of the most appealing aspects of the Bingham model is that one can use the dimensions of the final lava flow to estimate its rheology and thus composition through some very simple expressions (Moore 1978):

$$Y = \frac{\rho g H^2}{W_{flow}} \quad (1)$$

$$Y = 2\rho g \sin^2(a) W_{levee} \quad (2)$$

where

Y	is the yield strength;
W_{flow}	is width of the flow;
W_{levee}	is width of the levee;
g	is gravitational acceleration;
a	is slope;
H	is the thickness of the flow; and
ρ	is density.

Equations 1 and 2 have been used extensively in planetary science for many decades and have proven useful in classifying lavas as a relatively viscous fluid (Hulme, 1974). However, connecting the specific viscosity and yield strength numbers to laboratory measurements has proven problematic. The reason is straightforward; the laboratory measurements consider a small volume of uniform material, but the lava morphometry is affected by the bulk properties of the lava including the solidified outer crust and fluid interior. In detail, the Bingham model makes predictions that are inconsistent with how lava really behaves. In particular, the model predicts that levees form as low-standing stationary rims to a taller central part of the lava that moves downhill. In reality, the flow within the channel does not stand above the levees unless it is spilling out of the channel.

Stop 3. Lava Flow

Walk across the dirt road and onto the lava flow (fig. 22). When possible, walk along the vegetated portion of the flow, which tends to be relatively flat (fig. 32). The unvegetated, blocky flow comprises many loose blocks, which make a traverse across this portion of the flow difficult, time consuming, and potentially dangerous.

Goal.—Identify the different lava flow surface textures. Use your observations of the lava flow to help create a relative sequence of the different eruptive stages.

Task 1.—As you walk across the lava flow, take note of the different sizes, textures, and morphology of the tephra and lava flow blocks.

- What kind of information regarding the eruption can you gather from the different lava flow surface textures?
- How can you use such observations to determine the relative timing for lava emplacement?



Figure 32. Photograph taken on the vegetated portion of the lava flow at stop 3 looking to the south. Blue clipboard for scale. S P Mountain is in the background. Photograph by Amber Gullikson and M. Elise Rumpf, U.S. Geological Survey.

- Can the different surface textures represent lava emplaced at different times of the eruption?
- How might erosion affect lava flow features?
- If you were looking at a satellite photograph of a lava flow on the Moon or Mars, how could you use lava flow dimensions and surficial features to better understand the types of volcanism that occurred?

Summary.—The S P Mountain blocky lava flow erupted from the same central vent that formed S P Mountain. This flow displays two types of surface textures that have been described in detail in the “S P Mountain and its lava flow” section. As previously mentioned, the part of the lava flow that displays surface texture 1 in figure 33 is covered in vegetation and has a wide variety of clast sizes. It is covered in a thin layer of tephra, indicating that Hawaiian-style activity was still occurring when this phase of the flow erupted from the vent. Along the margins of the flow are



Figure 33. Photograph of surface texture 1 at stop 3. Surface texture 1 is typically vegetated and covered by tephra. Blue clipboard in the upper image and a pen in the lower image for scale. Photograph by Amber Gullikson and M. Elise Rumpf, U.S. Geological Survey.

large pieces of oxidized, agglutinated material, assumed to be remnants of the initial cone that was subsequently broken off and carried with the flow.

Areas of the flow displaying surface texture 2 comprise polyhedral blocks ranging in size from ~10 centimeters to as much as 1 m (fig. 34) (Hodges, 1962). This portion of the flow lacks the soil and vegetation that is characteristic of surface texture 1, and no oxidized, agglutinated material is observed. This suggests that this phase of the eruption was not destructive, that is, it did not carry away large fragments of near-vent material downstream. Distinct narrow channels of the blocky flow (surface texture 2) extend across the vegetated parts of the flow (surface texture 1) in an east-west direction, trending almost perpendicular to the direction of the main flow (in other words, to the north) (fig. 35) and indicating that this pulse of lava occurred after the initial lava flow eruption phase.

The last main feature highlighted at this stop has been described as polygonal pavement (fig. 36) (Hodges, 1960). Polygonal pavement refers to areas of the blocky lava flow that did not fully break apart when the lava cooled and contracted, but rather remained fitted together, resulting in a smooth, jointed surface (Hodges, 1960). The polygonal pavement can be seen on the west interior side of the main channel, less than 100 m from the road.



Figure 34. Photograph of a blocky and unvegetated lava flow (resembling surface texture 2), looking south from stop 3. S P Mountain is in the background. Blue clipboard for scale. Photograph by Amber Gullikson and M. Elise Rumpf, U.S. Geological Survey.



Figure 35. Photographs of the S P Mountain lava flow at stop 3. *A*, Shows a narrow channel of the blocky flow extending across the vegetated, soil-accumulated part of the flow. This narrow channel is nearly perpendicular to the main flow direction, in other words, flow direction is to the north and this channel trends east-west. *B*, Shows a location where remnants of the blocky flow pooled in place. Photographs by Amber Gullikson and M. Elise Rumpf, U.S. Geological Survey.

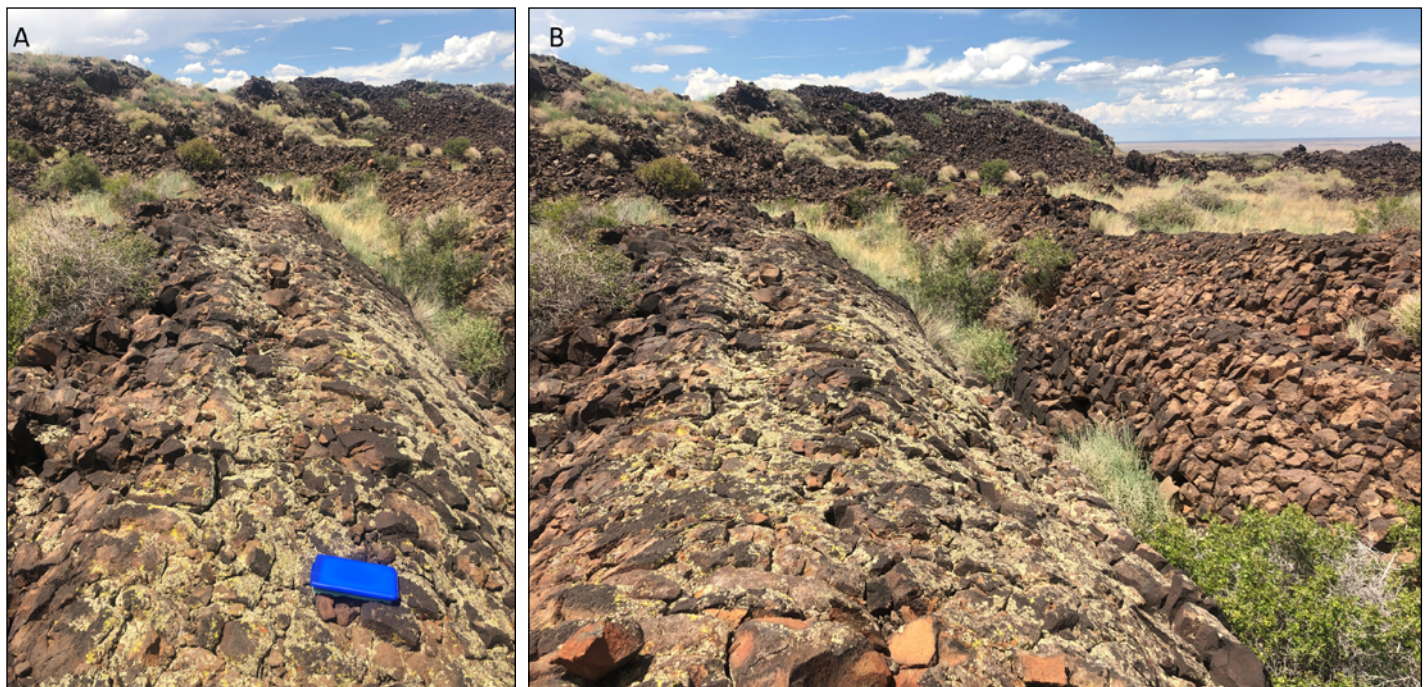


Figure 36. Photographs (A and B) of polygonal pavement at stop 3. Polygonal pavement are the areas of blocky lava flow that did not fully break apart when the lava cooled and contracted, but rather remained fitted together, resulting in a smooth, joined surface. Blue clipboard for scale in *A*. Photographs by Amber Gullikson and M. Elise Rumpf, U.S. Geological Survey.

Stop 4. The Rim of S P Mountain

Reaching this next stop requires a hike to the rim of S P Mountain. This is a strenuous hike. It is an 820 ft elevation gain over loose tephra and should only be done when one has plenty of water and the appropriate hiking attire. The easiest, most straightforward route is to begin at the contact between S P Mountain and the older tephra cone to the west, walking alongside the debris apron (fig. 30). Once you reach the saddle between these two cones, you will then begin the ascent on the west-facing side of S P Mountain. This preferred hiking path is shown in figure 22 by the white dashed line.

Goal 1.—Describe the rocks along the upper flanks and rim of S P Mountain. Hypothesize how the physical properties of these rocks might affect the preservation and (or) erosion of this volcano.

Goal 2.—Apply relative ages to the surrounding tephra cones based on their morphology.

Goal 3.—Identify the advantages and disadvantages of using remote sensing (for example, satellite imagery) versus being out in the field and vice versa.

Task 1.—As you hike S P Mountain, take note of the variability in tephra (for example, size, vesicularity, angularity, color, and so on). Does the tephra appear frothy in texture or welded? Look back to the descriptions of the different types of tephra at stop 1 and determine if both types appear on the upper flanks of S P Mountain. Is one type of tephra more prevalent here than the other?

Task 2.—Once at the top of S P Mountain, observe the inside of the crater and its rim. Do the rocks along the rim look similar to what composes the flanks of S P Mountain? What are the similarities? What are the differences? How might the physical properties of these volcanic rocks influence either the erosion and (or) preservation of S P Mountain?

Task 3.—Observe the various textures along the rim. Using the photographs in the guide, try to find other samples with similar textures, such as breadcrust, ropy, and banding. Are there other



Figure 37. Photograph taken at stop 4 of the rim of S P Mountain looking east. Global positioning system (GPS) coordinates, lat 35°34'59.3" N., long 111°38'01.1" W. Photograph by Amber Gullikson and M. Elise Rumpf, U.S. Geological Survey.

features or volcanic textures not discussed in the guide that you see?

Task 4.—Prior to leaving this stop, look at the lava flow from this vantage point and the surrounding tephra cones on all sides of S P Mountain. The surrounding volcanoes have varying levels of degradation. By observing the extent of erosion, apply approximate relative ages for each of the surrounding cones. What erosional mechanisms (for example, rain, wind, and so on) are likely to have played an important role in degrading these volcanoes?

Task 5.—Look to the S P Mountain lava flow. Can you identify the same features that you observed while standing on top of the lava flow (stop 3)? Are there additional observations that you can only see from this vantage point in comparison to standing directly on the flow?

Using satellite and aerial imagery of the area (figs. 16, 17, and 18):

- Are there features you can only identify using satellite and aerial images versus being out in the field?
- What challenges exist for identifying features in satellite images that are made easier in the field?
- What challenges exist for identifying features in the field that are made easier by looking at satellite images?
- How would this exercise differ when standing near stops 1 or 2, versus up here at the rim?

Summary.—The rim of S P Mountain comprises agglutinated material covered in a thin growth of vegetation (figs. 37 and 38). This agglutinated material is much more resistant to weathering in contrast to loose tephra, and therefore has helped preserve the rim of S P Mountain from



Figure 38. Photograph taken at stop 4 from the rim of S P Mountain looking north. In the foreground are agglutinated fragments that show various textures. In the background is the S P Mountain lava flow. Global positioning system (GPS) coordinates, lat 35°34'59.3" N., long 111°38'01.1" W. Photograph by Amber Gullikson and M. Elise Rumpf, U.S. Geological Survey.

erosion. Many of the volcanic clasts found along the rim display breadcrust and (or) ropy textures, very similar to what was previously seen at stop 1. Figure 39 shows an excellent example of red, agglutinated volcanic material having a ropy texture. This was likely the result of the lava being stretched while it was still partially molten and plastic, most likely while in motion traveling through the air. Figures 40 and 41 show examples of interesting volcanic textures found along the rim, including a lava bomb with welded-on lapilli and compressional bands, respectively.

Both surface textures of the lava flow can be observed here, as well as lobes of the flow that entered the graben (fig. 42). Several elongated and circular tephra cones surround S P Mountain. Two elongated cones parallel the S P Mountain lava flow to the east (fig. 43), in addition to one located to the southwest (fig. 44) and one to the southeast of S P Mountain. Nearly due south of S P Mountain is Colton Crater (fig. 45), a volcanic maar (low-relief, broad *volcanic* crater formed by shallow explosive eruptions. The explosions are usually caused by the heating and boiling of groundwater when magma begins to occupy the same space as the groundwater table [<https://volcanoes.usgs.gov/vsc/glossary/>]) with a resurgent dome on the crater floor. The thin layering that can be seen on the crater's interior walls represents numerous phreatomagmatic explosions, in which hot ash and tephra were deposited on the rim. After the main volcanic activity ceased, a resurgent dome built up on the crater's floor by a later stage of basaltic volcanism.



Figure 39. Photograph of a red agglutinated piece of volcanic rock taken on the rim of S P Mountain at stop 4. Near the field notebook is an example of ropy texture. Global positioning system (GPS) coordinates, lat 35°34'59.3" N., long 111°38'01.1" W. Photograph by Amber Gullikson and M. Elise Rumpf, U.S. Geological Survey.



Figure 40. Photograph of smaller lapilli welded onto a lava bomb taken along the rim of S P Mountain at stop 4. Photograph by Amber Gullikson and M. Elise Rumpf, U.S. Geological Survey.



Figure 41. Photograph of compressional bands on a volcanic rock taken along the rim of S P Mountain at stop 4. Pen for scale. Photograph by Amber Gullikson and M. Elise Rumpf, U.S. Geological Survey.



Figure 42. Photograph taken at stop 4 looking northwest toward the S P Mountain lava flow. The graben can be seen in the upper left part of the image, along with two lobes of the S P Mountain lava flow entering into the graben. Photograph by Amber Gullikson and M. Elise Rumpf, U.S. Geological Survey.

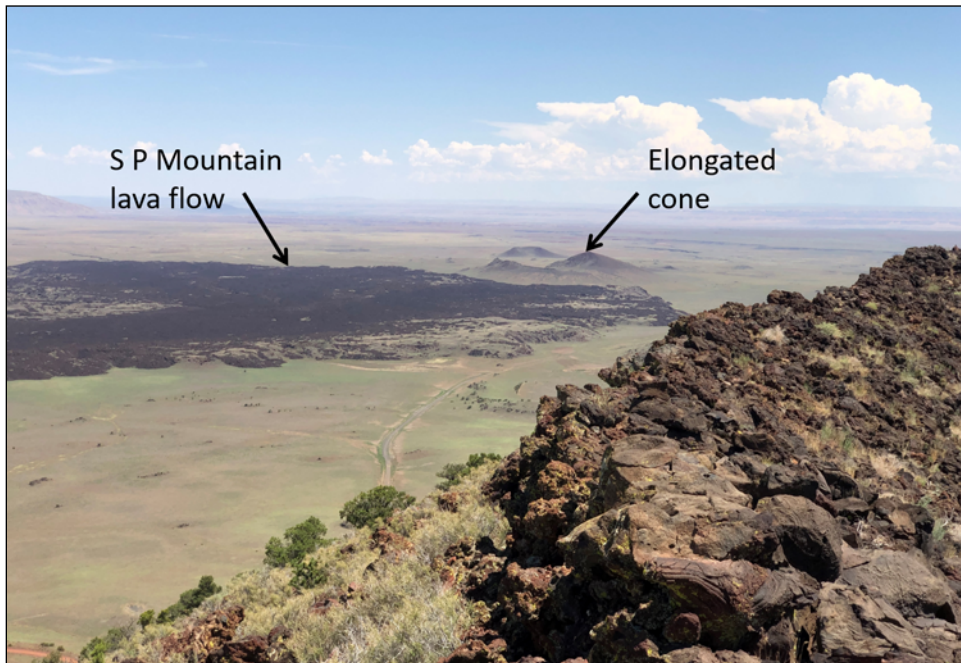


Figure 43. Photograph taken at stop 4 looking northeast. To the east of the S P Mountain lava flow is an elongated cone that formed along a fissure. Photograph by Amber Gullikson and M. Elise Rumpf, U.S. Geological Survey.

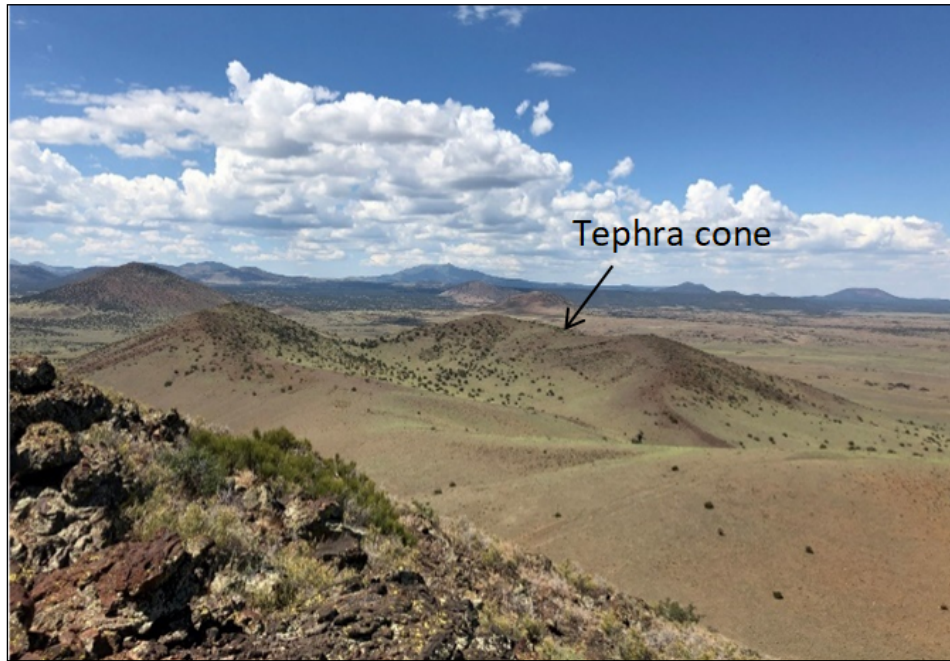


Figure 44. Photograph taken at stop 4 on the rim of S P Mountain looking southwest. The tephra cone centered in the image has a wide central crater with elongated rims. Global positioning system (GPS), lat 35°34'57.0" N., long 111°38'02.5" W. Photograph by Amber Gullikson and M. Elise Rumpf, U.S. Geological Survey.

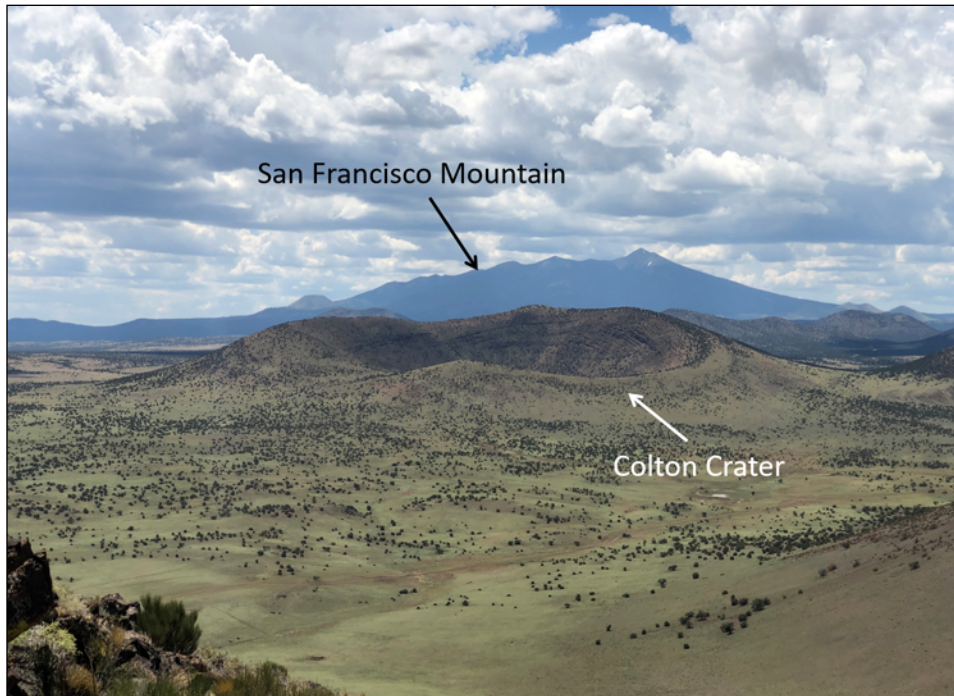


Figure 45. Photograph taken at stop 4 on the rim of S P Mountain looking to the south at Colton Crater. Photograph by Amber Gullikson and M. Elise Rumpf, U.S. Geological Survey.

Stop 5. Graben

Before proceeding, a four-wheel drive vehicle with high clearance and an experienced driver is needed to drive to stop 5. It can also be reached by foot from the original parking spot (the circle indicated in figure 22), or by driving farther west and parking off an unmarked dirt road (lat 35°36'10.1" N., long 111°38'46.0" W.) (fig. 46). Cacti are found throughout this area; therefore, appropriate hiking attire, such as closed-toed shoes and long pants are encouraged.

This stop highlights the graben and shows an excellent view of an unconformity between the Kaibab Limestone and the S P Mountain lava flow (fig. 47).

Lobes of the S P Mountain lava flow entered the graben along the fault in two locations. To reach this stop (and the closest of the two lobes), a brief drive over an older lava flow and a short hike are required (fig. 46). From the pull off where cars were originally parked, drive west for 0.84 miles (~1.34 km) and turn north on another unmarked dirt road (lat 35°35'30.1" N., long 111°38'58.2" W.). Drive 1 mile (1.6 km) north along this dirt road. Once you have gone this distance (lat 35°36'10.1" N., long 111°38'46.0" W.), pull onto the side of the road and begin hiking towards the contact point between the Kaibab Limestone and the S P Mountain lava flow, which should be approximately 0.27 miles (~440 m) to the ~east (lat 35°36'12.2" N., long 111°38'33.0" W.).

At this location, observe the contact between the S P Mountain lava flow and the Kaibab Limestone (fig. 47), as well as the lobe of the lava flow where it entered the graben. Numerous large agglutinated mounds that have been transported away from the central vent can be observed here (fig. 48). If you have enough time, you can hike up the lobe and onto the lava flow for additional views (figs. 49–51).



Figure 46. Satellite image showing how to get to stop 5. White circle is the parking location for stops 1 through 4. White star is the turnoff onto the unmarked dirt road (lat 35°35'30.1" N., long 111°38'58.2" W.); blue star is the suggested location to pull off and park (lat 35°36'10.1" N., long 111°38'46.0" W.); and red star is the location of stop 5 (lat 35°36'12.2" N., long 111°38'33.0" W.). Basemap is by Esri, Maxar Technologies, GeoEye, Earthstar Geographics, CNES.Airbus DS, U.S. Department of Agriculture (USDA) Farm Service Agency, U.S. Geological Survey (USGS), AeroGRID, IGN, and the GIS User Community, data served by Esri web service (https://services.arcgisonline.com/ArcGIS/rest/services/World_Imagery/MapServer), Map data 2021.

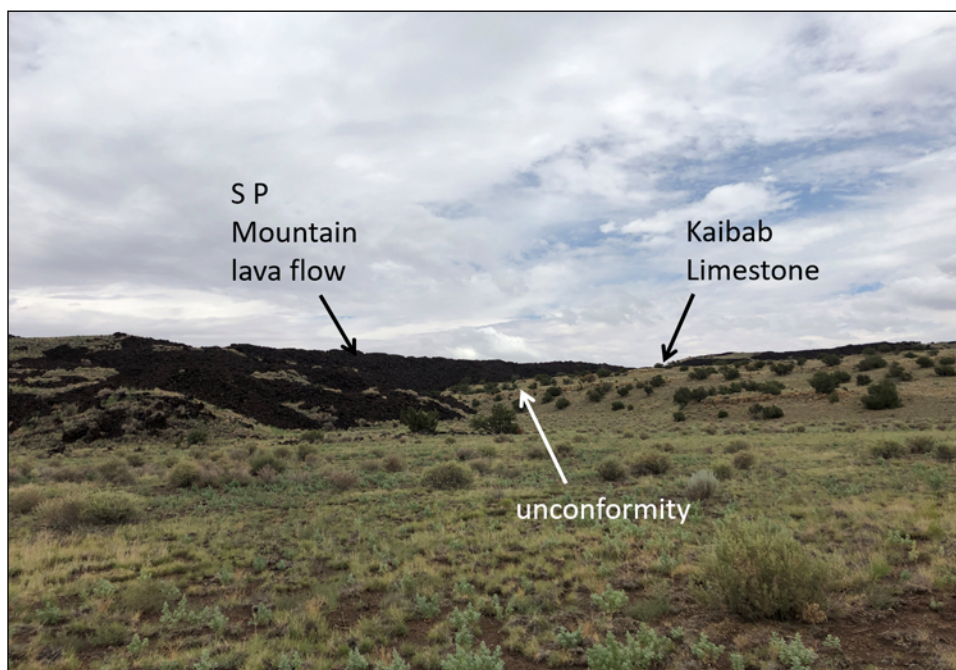


Figure 47. Photograph taken at stop 5 on the floor of the graben, looking northeast, with the S P Mountain lava flow superposing Kaibab Limestone. Global positioning system (GPS) coordinates, lat 35°36'08.6" N., long 111°38'43.3" W. Photograph by Amber Gullikson and M. Elise Rumpf, U.S. Geological Survey.

Figure 48. Photographs of agglutinated transported material located within the S P Mountain lava flow, taken at one of the lobes that entered the graben at stop 5. Photographs by Amber Gullikson and M. Elise Rumpf, U.S. Geological Survey.



Figure 49. Photograph at stop 5 between the Kaibab Limestone (right) and the S P Mountain lava flow (left). Measuring tape in the center of image is 50 centimeters in length. Global positioning system (GPS) coordinates, lat 35°36'13.1" N., long 111°38'31.9" W. Photograph by Amber Gullikson and M. Elise Rumpf, U.S. Geological Survey.

Goal 1.—Determine relative ages of the graben and S P Mountain lava flow.

Goal 2.—Determine the environmental setting of this area when the Kaibab Limestone was deposited.

Task 1.—Is the formation of the graben older or younger than the S P Mountain lava flow? What do you notice about the thickness of the lava flow above the graben versus inside the graben? Which surface texture of the lava flow (one or both) is observed at this location? Can you identify which surface texture is responsible for transporting the agglutinated material?

Task 2.—The Kaibab Limestone is ~270 Ma and the age of S P Mountain is less than 70 ka. Why is there such a time gap between the two units? What type of environment was this area when the Kaibab Limestone was deposited? What kind of environment was this area when S P Mountain was erupting? What type of clues could you use to help answer this?

Summary.—Using crosscutting relationships and the law of superposition, we can formulate a relative sequence of events at this location. The fault movement that resulted in the formation of the graben cuts through and offsets the Kaibab Limestone. Therefore, the Kaibab Limestone must predate the faults that cut through it. The law of superposition informs us that younger rocks typically superpose or cover older rocks. The S P Mountain lava flow both covers the Kaibab Limestone and flows into the graben, therefore indicating that the S P Mountain flow is younger than both the Kaibab Limestone and the graben.



Figure 50. Photograph of the S P Mountain lava flow lobe, taken standing on the Kaibab Limestone looking south at stop 5. The lava flow is very blocky at this location, and the core of it is exposed. The lava flow transported the agglutinated material that came to a rest here as well. Global positioning system (GPS) coordinates, lat 35°36'13.8" N., long 111°38'29.8" W. Photograph by Amber Gullikson and M. Elise Rumpf, U.S. Geological Survey.



Figure 51. Photograph of the S P Mountain lava flow on the left side with S P Mountain in the background, taken looking south, standing on top of an agglutinated mound transported by the S P Mountain lava flow. Photograph by Amber Gullikson and M. Elise Rumpf, U.S. Geological Survey.

The formation of limestone indicates that this area was a shallow seafloor at one point in time. The Kaibab Limestone spans across parts of northern Arizona, southern Utah, Nevada, and California, and comprises carbonate and siliciclastic sediments, with lesser amounts of dolomite and chert. The complex-interfingering relationships of these various sediments indicate that at the time of deposition, sea levels were changing.

Younger sediments were subsequently deposited but have since eroded. At the onset of San Francisco Volcanic Field volcanism, erosion had exposed the Kaibab Limestone. As volcanism occurred across the area, younger volcanic rocks were deposited over the older Kaibab Limestone resulting in an unconformity.

Questions for Discussion at the End of the Field Trip

Compare the features that you observed on the ground, at a vantage point (for example, rim of S P Mountain), and satellite images.

- If you wanted to solely use remote sensing to observe these same features, how high would the image resolution need to be?
- What types of capabilities or instruments do we have for other planets?
- Can we see similarly sized features to those we have observed here on the surface of Mars or the Moon? If so, using what kind of instruments? If not, why not?
- What kind of information might be missing from remote-based observations?
- What kind of information might be missing from ground-based observations? How specifically might these affect our interpretations?

There are volcanic features very similar to what we have seen throughout this field guide on both Mars and the Moon. Imagine yourself on another planet, hiking along a lava flow or up the steep flanks of a volcano (like you just accomplished).

- If you had to wear a thick astronaut suit, comparable to those used during the Apollo missions, how easy would it be to replicate what you just did?
- What types of hazards might you run into hiking along this type of terrain on another planet?
- What types of hazards and traverse limitations would need to be considered when using a rover on this type of terrain?
- How would factors like gravity or atmospheric thickness affect you and your rover's capabilities?

References

- Alexander, C.M.O'D., and Wetherill, G.W., 2020, Meteorite: Encyclopedia Britannica website, accessed May 24, 2021, at <https://www.britannica.com/science/meteorite>.
- Arculus, R.J., and Gust, D.A., 1995, Regional petrology of the San Francisco Volcanic Field, Arizona, USA: *Journal of Petrology*, v. 36, no. 3, p. 827–861.
- Babenroth, D.L., and Strahler, A.N., 1945, Geomorphology and structure of the East Kaibab monocline, Arizona and Utah: *Bulletin of the Geological Society of America*, v. 56, p. 107–150.
- Barnett, A., Glaze, L., Erickson, K., McLaurin, L., and Dunford, B., 2018, Vesta, Vesta Science—NASA Solar System Exploration, accessed May 24, 2021, at <https://solarsystem.nasa.gov/missions/dawn/science/vesta/>.
- Baski, A.K., 1974, K-Ar study of the S P Flow: *Canadian Journal of Earth Sciences*, v. 11, no. 10, p. 1350–1356.
- Billingsley, G.H., Breed, W.J., and Beasley, D., 1980, Geologic cross section along Interstate 40—Kingman to Flagstaff, Arizona: Petrified Forest Museum Association, 2 sheets.
- Bloomfield, A.L., and Arculus, R.J., 1989, Magma mixing in the San Francisco Volcanic Field, AZ: Petrogenesis of the O'Leary Peak and Strawberry Crater Volcanics: *Contributions to Mineralogy and Petrology*, v. 102, p. 429–453.
- Bradley, B.A., Sakimoto, S.E.H., Frey, H., and Zimbelman, J.R., 2002, Medusae Fossae Formation—New perspectives from Mars Global Surveyor: *Journal of Geophysical Research*, v. 107.
- Brož, P., and Hauber, E., 2012, A unique volcanic field in Tharsis, Mars—Pyroclastic cones as evidence for explosive eruptions: *Icarus*, v. 218, no. 1, p. 88–99.
- Campbell, B.A., Hawke, B.R., and Campbell, D.B., 2009, Surface morphology of domes in the Marius Hills and Mons Rümker regions of the Moon from Earth-based radar data: *Journal of Geophysical Research Planets*, v. 114, no. E1, p. 1–10.
- Carr, M.H., 1973, Volcanism on Mars: *Journal of Geophysical Research*, v. 78, p. 4049–4062.
- Cattermole, P. J., 1989, Planetary volcanism—A study of volcanic activity in the solar system: Chichester, E. Horwood; New York: Wiley, 443 p.
- Chen, W., and Arculus, R.J., 1995, Geochemical and isotopic characteristics of lower crustal xenoliths, San Francisco Volcanic Field, Arizona, USA: *Lithos*, v. 36, p. 203–225.
- Christensen, P.R., Gorelick, N.S., Mehall, G.L., and Murray, K.C., THEMIS Public Data Releases, Planetary Data System node, Arizona State University, accessed July 9, 2021, at <https://themis-data.asu.edu>.

- Colton, H.S., 1936, The basaltic cinder cones and lava flows of the San Francisco Mountain volcanic field: Flagstaff, Arizona—Museum of Northern Arizona, 58 p.
- Connor, C.B., Condit, C.D., Crumpler, L.S., and Aubele, J.C., 1992, Evidence of regional structural controls on vent distribution—Springer volcanic field, Arizona: *Journal of Geophysical Research*, v. 100, p. 10107–10125.
- Conway, F.M., Connor, C.B., Hill, B.E., Condit, C.D., Mullaney, K., and Hall, C.M., 1998, Recurrence rates of basaltic volcanism in S P cluster, San Francisco Volcanic Field, Arizona: *Geology*, v. 26, no. 7, p. 655–658.
- Conway, F.M., Ferrill, D.A., Hall, C.M., Morris, A.P., Stamatakos, J.A., Connor, C.B., Halliday, A.N., and Condit, C., 1997, Timing of basaltic volcanism along the Mesa Butte fault in the San Francisco Volcanic Field, Arizona, from $^{40}\text{Ar}/^{39}\text{Ar}$ dates—Implications for longevity of cinder cones alignments: *Journal of Geophysical Research*, v. 102, p. 815–824.
- Cooley, M.E., 1962, Geomorphology and age of volcanic rocks in northeastern Arizona: *Arizona Geological Society Digest*, v. 5, p. 97–115.
- Crow, R., Karlstrom, K., Asmerom, Y., Schmandt, B., Polyak, V., and DuFrane, S.A., 2011, Shrinking of the Colorado Plateau via lithospheric mantle erosion—Evidence from Nd and Sr isotopes and geochronology of Neogene basalts: *Geology*, v. 39, no. 1, p. 27–30.
- Davis, G.H., and Bump, A.P., 2009, Structural geologic evolution of the Colorado Plateau, in Kay, S.M., Ramos, V.A., and Dickinson, W.R., eds., *Backbone of the Americas—Shallow subduction, plateau uplift, and ridge and terrane collision*: Geological Society of America Memoir 204, p. 99–124.
- Fenneman, N.M., and Johnson, D.W., 1946, Physical divisions of the United States: U.S., Geological Survey, scale 1:7,000,000, 1 sheet.
- Fenton, C.R., and Niedermann, S., 2014, Surface exposure dating of young basalts (1–200 ka) in the San Francisco Volcanic Field (Arizona, USA) using cosmogenic ^3He and ^{21}Ne : *Quaternary Geochronology*, v. 19, p. 87–105.
- Greeley, R., and Spudis, P.D., 1981, Volcanism on Mars: *Reviews of Geophysics*, v. 19, p. 13–41.
- Gregg, T.K.P., Lopes, R.M., and Fagents, S.A., 2020, *Planetary volcanism across the solar system*: Elsevier, 400 p.
- Harmon, J.K., Nolan, M.C., Husmann, D.I., and Campbell, B.A., 2012, Arecibo radar imagery of Mars: The major volcanic provinces: *Icarus*, v. 220, p. 990–1030.
- Hodges, C.A., 1962, Comparative study of S P and Sunset Craters and associated lava flows, San Francisco Volcanic Field, Arizona: University of Wisconsin, M.S. thesis.
- Hodges, C.A., and Moore, H.J., 1994, Atlas of volcanic landforms on Mars: U.S. Geological Survey Professional Paper 1534, 194 p.
- Holm, R.F., 1987, Significance of agglutinate mounds on lava flows associated with monogenic cones—An example of Sunset Crater, northern Arizona: *Geological Society of America Bulletin*, v. 99, p. 319–324.
- Hulme, G., 1974, The interpretation of lava flow morphology: *Geophysical Journal of the Royal Astronomical Society*, v. 39, p. 361–383.
- Humphreys, E.D., 1995, Post-Laramide removal of the Farallon slab, western United States: *Geology*, v. 23, no. 11, p. 987–990.
- Humphreys, E.D., Hessler, E., Dueker, K., Farmer, G.L., Erslev, E., and Atwater, T., 2003, How Laramide-age hydration of North American lithosphere by the Farallon slab controlled subsequent activity in the western United States: *International Geology Review*, v. 45, no. 7, p. 575–595.
- Huntington, K.W., Wernicke, B.P., and Eiler, J.M., 2010, Influence of climate change and uplift on Colorado Plateau paleotemperatures from carbonate clumped isotope thermometry: *Tectonics*, v. 29, 19 p.
- Jourdan, F., Kennedy, T., Benedix, G.K., Eroglu, E., and Mayer, C., 2020, Timing of the magmatic activity and upper crustal cooling of differentiated asteroid 4 Vesta: *Geochimica et Cosmochimica Acta*, v. 273, p. 205–225.
- Karlstrom, K.E., Crow, R., Crossey, L.J., Coblenz, D., and van Wijk, J.W., 2008, Model for tectonically driven incision of the younger than 6 Ma Grand Canyon: *Geology*, v. 36, p. 835–838.
- Kennedy, J.R., Paretto, N.V., and Veilleux, A.G., 2015, Methods for estimating magnitude and frequency of 1-, 3-, 7-, 15-, and 30-day flood-duration flows in Arizona (ver. 1.1, April 2015): U.S. Geological Survey Scientific Investigations Report 2014–5109, 35 p., accessed May 24, 2021, at <http://dx.doi.org/10.3133/sir20145109>.
- Kerber, L., Forget, F., Madeleine, J.-B., Wordsworth, R., Head, J.W., and Wilson, L., 2013, The effect of atmospheric pressure on the dispersal of pyroclasts from martian volcanoes: *Icarus*, v. 223, p. 149–156.
- Kereszturi, G., and Németh, K., 2012, Monogenetic basaltic volcanoes—Genetic classification, growth, geomorphology and degradation, K. Németh (Ed.): *Updates in Volcanology—New Advances in Understanding Volcanic Systems*: Intech Open, 11 p.
- Keszthelyi, L., 1995, A preliminary thermal budget for lava tubes on the Earth and planets: *Journal of Geophysical Research*, v. 100, p. 20411–20420.

- Keszthelyi, L., Jaeger, W., McEwen, A., Tornabene, L., Beyer, R.A., Dundas, C., and Milazzo, M., 2008, High Resolution Imaging Experiment (HiRISE) images of volcanic terrains from the first 6 months of the Mar Reconnaissance Orbiter Primary Science Phase: *Journal of Geophysical Research*, v. 113, 25 p.
- Keszthelyi, L., Self, S., and Thordarson, T., 2006, Flood lavas on Earth, Io, and Mars: *Journal of the Geological Society, London*, v. 163, p. 253–264.
- Keszthelyi, L., Thordarson, Th., McEwen, A., Haack, H., Guilbaud, M.-N., Self, S., and Rossi, M.J., 2004, Icelandic analogs to Martian flood lavas: *Geochemistry, Geophysics, Geosystems*, v. 5, 32 p.
- Levander, A., Schmandt, B., Miller, M.S., Liu, K., Karlstrom, K.E., Crow, R.S., Lee, C.-T.A., and Humphreys, E.D., 2011, Continuing Colorado Plateau uplift by delamination-style convective lithospheric downwelling: *Nature*, v. 472, p. 461–466.
- Lopes, R.M.C., and Gregg, T.K.P., 2004, *Volcanic worlds exploring the solar system's volcanoes*: Springer Praxis Books, 236 p.
- Luedke, R.G., and Smith, R.L., 1978, Map showing distribution, compositions, and age of late Cenozoic volcanic centers in Arizona and New Mexico. U.S. Geological Survey Miscellaneous Investigation Series Map I-1091-A, scale 1:1,000,000.
- McQuarrie, N., and Chase, C.G., 2000, Raising the Colorado Plateau: *Geology*, v. 28, no. 1, p. 91–94.
- Mooney, W.D., Laske, G., and Masters, T.G., 1998, Crust 5.1: A global crustal model at 5°x5°: *Journal of Geophysical Research*, v. 103, p. 10,049–10,077.
- Moore, H.J., Arthur, D.W.G., and Schaber, G.G., 1978, Yield strengths of flows on the Earth, Mars, and Moon: *Proceedings of the 9th Lunar and Planetary Science Conference*, Houston, TX, p. 3351–3378.
- Moore, R.B. and Wolfe, E.W., 1987, Geologic map of the east part of the San Francisco Volcanic Field, north-central Arizona: U.S. Geological Survey Miscellaneous Field Studies Map MF-1960, scale 1:50,000.
- Moore, R.B., Wolfe, E.W., Ulrich, G.E., 1976, Volcanic rocks of the eastern and northern parts of the San Francisco Volcanic Field, Arizona: *Journal of Research*, v. 4, no. 5 p. 549–560.
- Morgan, P., and Swanberg, C.A., 1985, On the Cenozoic uplift and tectonics stability of the Colorado Plateau: *Journal of Geodynamics*, v. 3, p. 39–63.
- Moucha, R., Forte, A.M., Rowley, D.B., Mitrovica, J.X., Simmons, N.A., and Grand, S.P., 2008, Mantle convection and the recent evolution of the Colorado Plateau and the Rio Grande Rift valley: *Geology*, v. 36, no. 6, p. 439–442.
- Moucha, R., Forte, A.M., Rowley, D.B., Mitrovica, J.X., Simmons, N.A., and Grand, S.P., 2009, Deep mantle forces and the uplift of the Colorado Plateau: *Geophysical Research Letters*, v. 36, 6 p.
- Mullaney, K.M., 1996, The petrology and geochemistry of lava from cinder cones along alignments in the S P region of the San Francisco Volcanic Field, Arizona [M.S. thesis]: Amherst, University of Massachusetts, 169 p.
- Newhall, C.G., and Self, S., 1982, The Volcanic Explosivity Index (VEI)—An estimate of explosive magnitude for historical volcanism: *Journal of Geophysical Research*, v. 87, p. 1231–1238.
- Newhall, C.G., Ulrich, G.E., and Wolfe, E.W., 1987, Geologic map of the southwest part of the San Francisco Volcanic Field, north-central Arizona: U.S. Geological Survey Miscellaneous Field Studies Map MF-1958, scale 1:24,000.
- Ort, M.H., Elson, M.D., and Champion, D.E., 2002, A paleomagnetic dating study of Sunset Crater Volcano: *Desert Archaeology Technical Report 2002-16*, 16 p.
- Reid, M.R., Bouchet, R.A., Blichert-Toft, J., Levander, A., Liu, K., Miller, M.S., and Ramos, F.C., 2012, Melting under the Colorado Plateau: *Geology*, v. 40, p. 387–390.
- Riggs, N.R., and Duffield, W.A., 2008, Record of complex scoria cone eruptive activity at Red Mountain, Arizona, USA, and implications for monogenetic mafic volcanoes: *Journal of Volcanology and Geothermal Research*, v. 178, p. 763–776.
- Rittenour, T.M., Riggs, N.R., and Kennedy, L.E., 2012, Application of single-grain OSL to date quartz xenocrysts within a basalt flow, San Francisco Volcanic Field, northern Arizona, USA: *Quaternary Geochronology*, v. 10, p. 300–307.
- Roberts, G.G., White, N.J., Martin-Brandis, G.L., and Crosby, A.G., 2012, An uplift history of the Colorado Plateau and its surroundings from inverse modeling of longitudinal river profiles: *Tectonics*, v. 31, 25 p.
- Robinson, H.S., 1913, The San Franciscan Volcanic Field, Arizona: U.S. Geological Survey Professional Paper 76, 213 p.
- Robson, S.G., and Banta, E.R., 1995, *Groundwater atlas of the United States, Arizona, Colorado, New Mexico, Utah*: U.S. Geological Survey Hydrologic Atlas 730-C, 32 p.
- Sabels, B.E., 1960, Late Cenozoic volcanism in the San Francisco Volcanic Field and adjacent areas in north central Arizona [Ph.D. Dissertation]: University of Arizona.
- Schaber, G.G., Elachi, C., and Farr, T.G., 1980, Remote sensing data of S P Mountain and S P lava flow in north-central Arizona: *Remote Sensing of Environment*, v. 9, p. 149–170.
- Shand, S.J., 1943, *Eruptive rocks*: New York: John Wiley and Sons, 444 p.

- Shoemaker, E.M., Squires, R.L., and Abrams, M.J., 1978, Bright Angel and Mesa Butte fault systems of northern Arizona: Geological Society of America Memoir 152, p. 341-367.
- Solomon, S.C., Nittler, L.R., and Anderson, B.J., 2018, Mercury—The view after MESSENGER, Cambridge University Press, 583 p.
- Spencer, J.E., 1996, Uplift of the Colorado Plateau due to lithosphere attenuation during Laramide low-angle subduction: *Journal of Geophysical Research*, v. 101, no. B6, p. 13,595–13,609.
- Spudis, P.D., 2015, Volcanism on the Moon, *The Encyclopedia of Volcanoes (Second Edition)*: Elsevier Inc., Amsterdam, Netherlands, Academic Press. p. 689–700.
- Tanaka, K.L., Shoemaker, E.M., Ulrich, G.E., and Wolfe, E.W., 1986, Migration of volcanism in the San Francisco Volcanic Field, Arizona: *Geological Society of America Bulletin*, v. 97, p. 129–141.
- Tanaka, K.L., Onstott, T.C., and Shoemaker, E.M., 1991, Magnetostratigraphy of the San Francisco Volcanic Field, Arizona: *U.S. Geological Survey Bulletin* 1929, 35 p.
- Tanaka, K.L., Skinner, J.A. Jr., Dohm, J.M., Irwin, R.P., III, Kolb, E.J., Fortezzo, C.M., Platz, T., Michael, G.G., and Hare, T.M., 2014, Geologic map of Mars: U.S. Geological Survey Scientific Investigations Map 3292, 1:20,000,000 scale.
- Ulrich, G.E., and Bailey, N.G., 1987, Geologic map of the S P Mountain part of the San Francisco Volcanic Field, north-central Arizona: U.S. Geological Survey Miscellaneous Field Studies Map MF-1956, 1:50,000 scale.
- Ulrich, G.E., Billingsley, G.H., Hereford, R., Wolfe, E.W., Nealey, L.D., Sutton, R.L., 1984, Map showing geology, structure, and uranium deposits of the Flagstaff 1°×2° quadrangle, Arizona: U.S. Geological Survey Miscellaneous Investigation Series Map I-1446, 1:50,000 scale.
- Valentine, G.A., and Connor, C.B., 2015, Basaltic volcanic fields chap. *in* *The Encyclopedia of Volcanoes (2d ed.)*: Elsevier Inc. Amsterdam, Academic Press, p. 423–439.
- Van Wijk, J.W., Baldrige, W.S., van Hunen, J., Goes, S., Aster, R., Coblenz, D.D., Grand, S.P., and Ni, J., 2010, Small-scale convection at the edge of the Colorado Plateau—Implications for topography, magmatism, and evolution of Proterozoic lithosphere: *Geology*, v. 38, no. 7, p. 611–614.
- Weikart, J.L., Seligman, A., Riggs, A.N., 2008, Origin of agglutinate material on the S P Crater lava flow and implications for eruptive history of a “simple” cinder cone, San Francisco Volcanic Field, northern Arizona: *Geological Society of America Abstracts with Programs* 40, p. 264.
- Wilson, L., and Head, J.W., 1981, Ascent and eruption of basaltic magma on the Earth and Moon: *Journal of Geophysical Research*, v. 86, p. 2971–3001.
- Wolfe, E.W., Ulrich, G.E., Holm, R.F., Moore, R.B., and Newhall, C.G., 1987a, Geologic map of the central part of the San Francisco Volcanic Field, north-central Arizona: U.S. Geological Survey Miscellaneous Field Studies Map MF-1959, scale 1:50,000.
- Wolfe, E.W., Ulrich, G.E., and Newhall, C.G., 1987b, Geologic map of the northwest part of the San Francisco Volcanic Field, north-central Arizona: U.S. Geological Survey Miscellaneous Field Studies Map MF-1957, 1:50,000 scale.
- Zandt, G., Myers, S.C., and Wallace, T.C., 1995, Crust and mantle structure across the Basin and Range-Colorado Plateau boundary at 37°N latitude and implications for Cenozoic extensional mechanisms: *Journal of Geophysical Research*, v. 100, p. 10,529–10,548.

